Supporting Information

Targeting the Alternative Vitamin E Metabolite Binding Site Enables Noncanonical PPARγ Modulation

Silvia Arifi[1], Julian A. Marschner[2], Julius Pollinger[1], Laura Isigkeit[1], Pascal Heitel[1], Astrid Kaiser[1], Lennart Obeser[2], Georg Höfner[2], Ewgenij Proschak[1,3], Stefan Knapp[1,4], Apirat Chaikuad[1,4], Jan Heering[3], Daniel Merk[1,2]*

[1] Institute of Pharmaceutical Chemistry, Goethe University Frankfurt, D-60438 Frankfurt, Germany
[2] Department of Pharmacy, Ludwig-Maximilians-Universität München, D-81377 Munich, Germany
[3] Fraunhofer Institute for Translational Medicine and Pharmacology ITMP, D-60596 Frankfurt, Germany
[4] Structural Genomics Consortium, BMLS, Goethe University Frankfurt, D-60438 Frankfurt, Germany
* daniel.merk@cup.lmu.de

Table of Contents

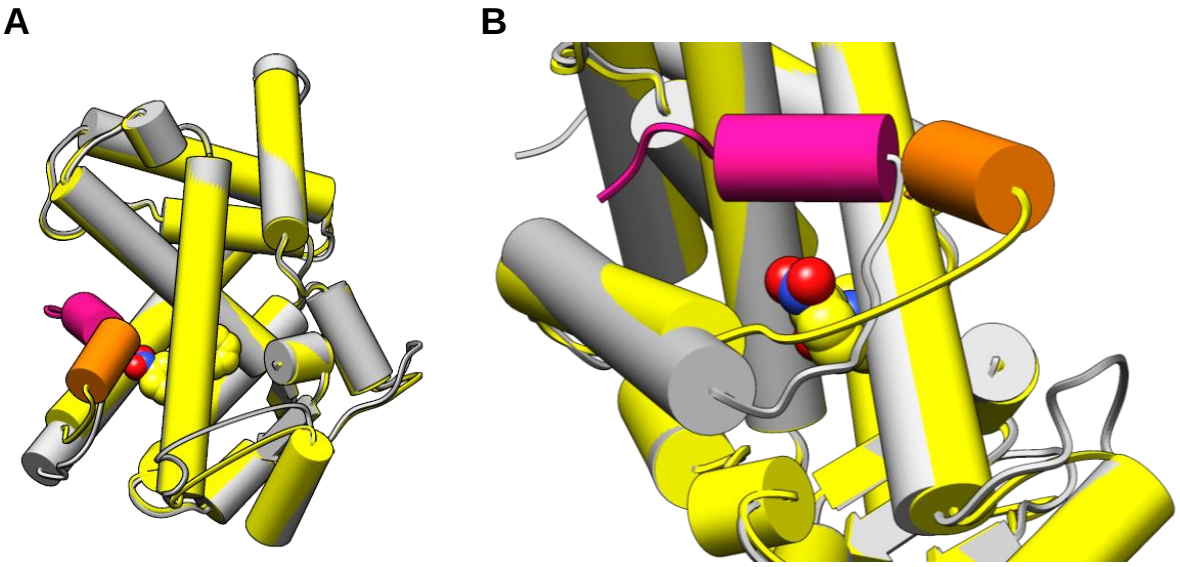

Figure S1. Structural comparison of the PPARγ LBD in complex with the agonist rosiglitazone (pdb ID: 7awc; protein grey, helix 12 magenta, ligand not shown) or the irreversible antagonist GW9662 (pdb ID: 3b0r, protein yellow, helix 12 orange, ligand yellow). The GW9662-bound PPARγ LBD conformation differs from the agonist bound state and reveals a shifted position of helix 12 which is due to a lack of helix 12 stabilization by the antagonist. However, GW9662 does not extend to or interfere with the active position of helix 12 indicating that activation via alternative mechanisms is not blocked by antagonist.

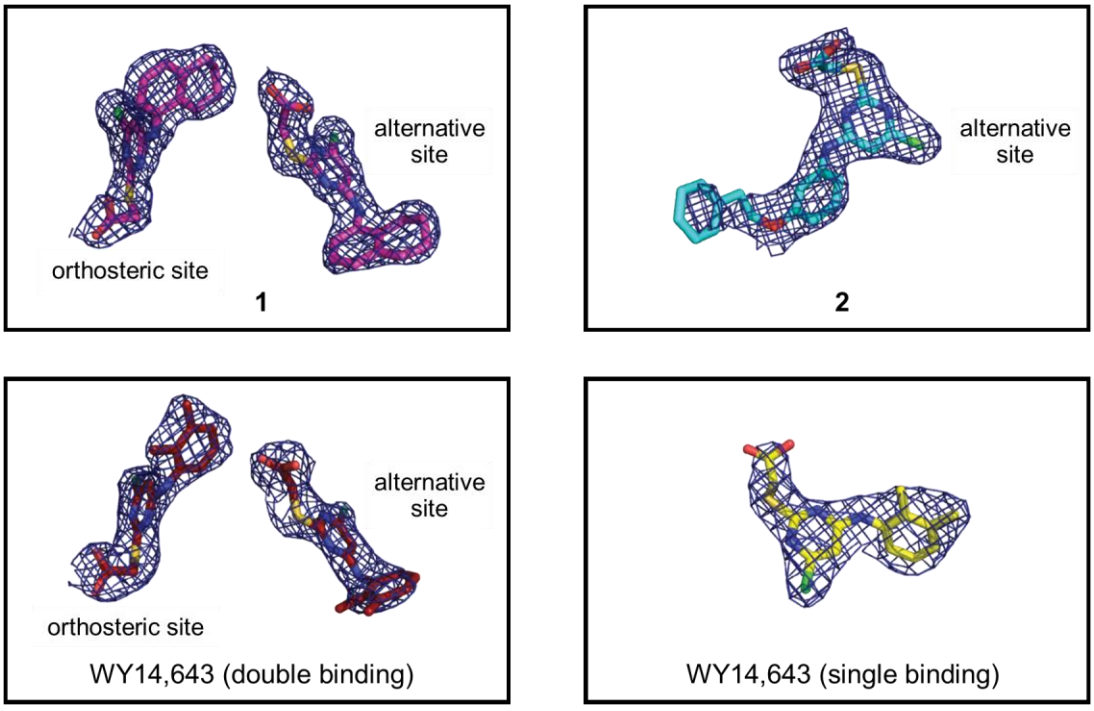

Figure S2. 2Fo-Fc electron density maps contoured at 1σ for **1** (pdb ID: 8aty), **2** (pdb ID: 8atz), and WY14,643 (pdb IDs: 8cpi, 8cph) bound to the PPARγ-LBD.

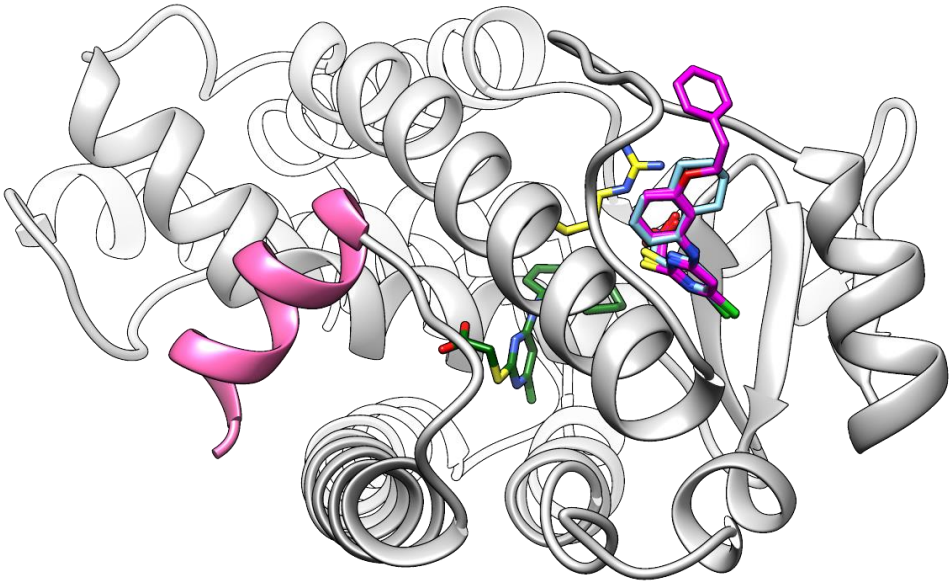

Figure S3. The PPARγ-**1** complex (pdb ID: 8aty; orthosteric site **1** - green, alternative site **1** - blue) indicated an opportunity to obtain selective binders of the alternative site by extension from the solvent exposed tetrahydronaphthalene motif of **1**. Compound **2** was designed based on this observation. Docking of **2** (magenta) into the alternative binding site of **1** supported this design hypothesis.

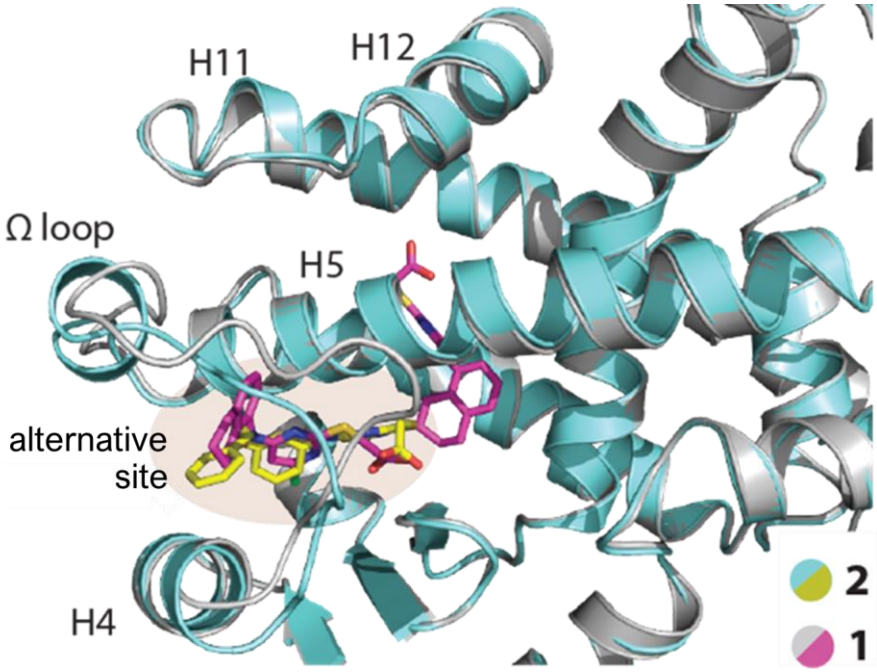

Figure S4. Superposition of the PPARγ LBD co-crystal structures in complex with **1** (magenta, pdb ID: 8aty) and **2** (yellow, pdb ID: 8atz) revealed highly similar active conformations but selective alternative site binding of **2**.

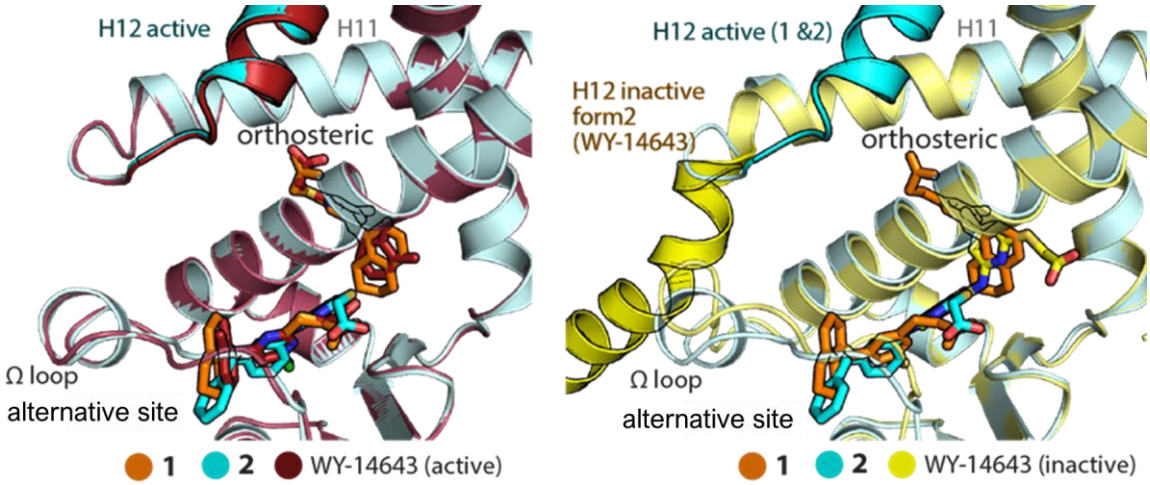

Figure S5. WY14,643 exhibits two diverse modes of binding to PPARγ. Double binding of WY14,643 to the orthosteric and alternative sites resembled the binding of **1** and induced an active conformation. Single binding of WY14,643, in contrast was observed similar to the binding of MRL-871 between the orthosteric and alternative sites in an inactive PPARγ conformation. PPARγ LBD bound to **1** (orange, pdb ID: 8aty) and **2** (blue, pdb ID: 8atz) for comparison.

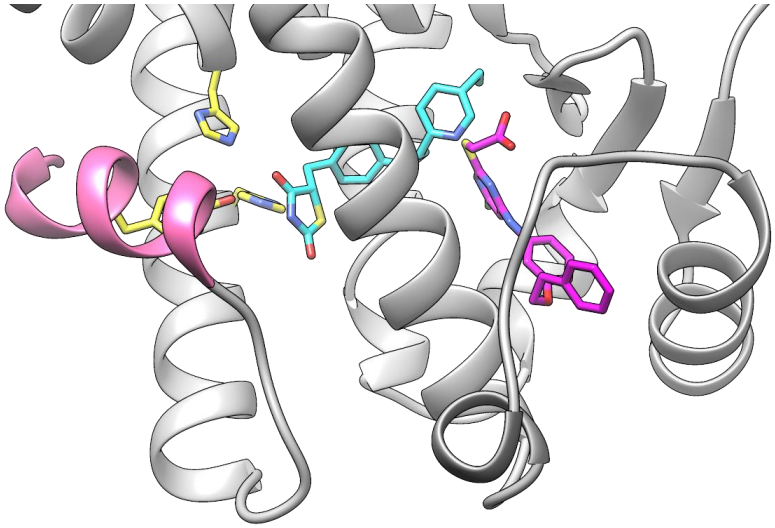

Figure S6. Molecular modeling supported simultaneous binding of pioglitazone (cyan) and **2** (magenta) to the PPARγ LBD. Pioglitazone was docked into the unoccupied orthosteric site of the PPARγ LBD bound to **2** (pdb ID: 8atz).

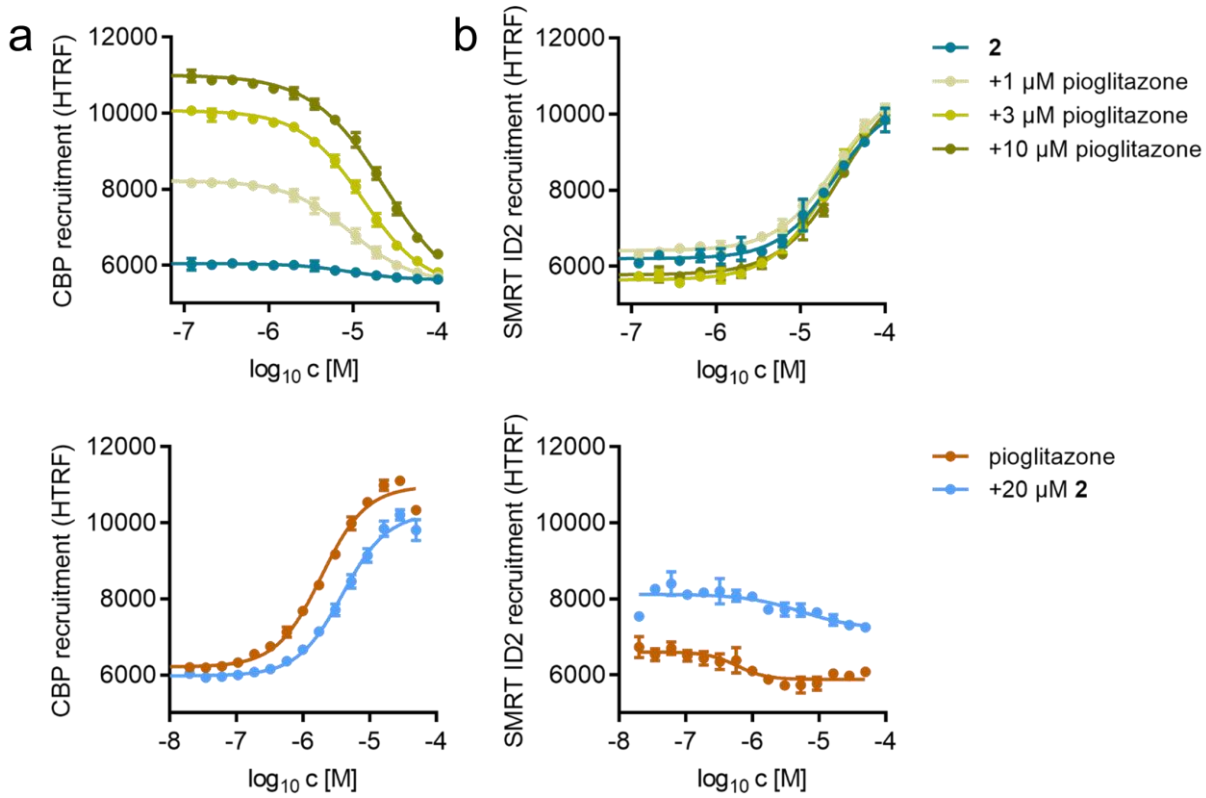

Figure S7. **2** dose-dependently modulates recruitment of co-regulators CBP (a) and SMRT-ID2 (b). Pioglitazone-stimulated recruitment of CBP was diminished by **2** in a dose-dependent manner, whereas **2** promoted recruitment of SMRT-ID2. 12 nM of biotin-labeled CBP or SMRT-ID2 peptide were coupled to 12 nM Tb-SA, and presented with sGFP-PPARγ LBD at either 100 nM (for CBP) or 24 nM (for SMRT-ID2). Data are the mean±SD HTRF; N=3.

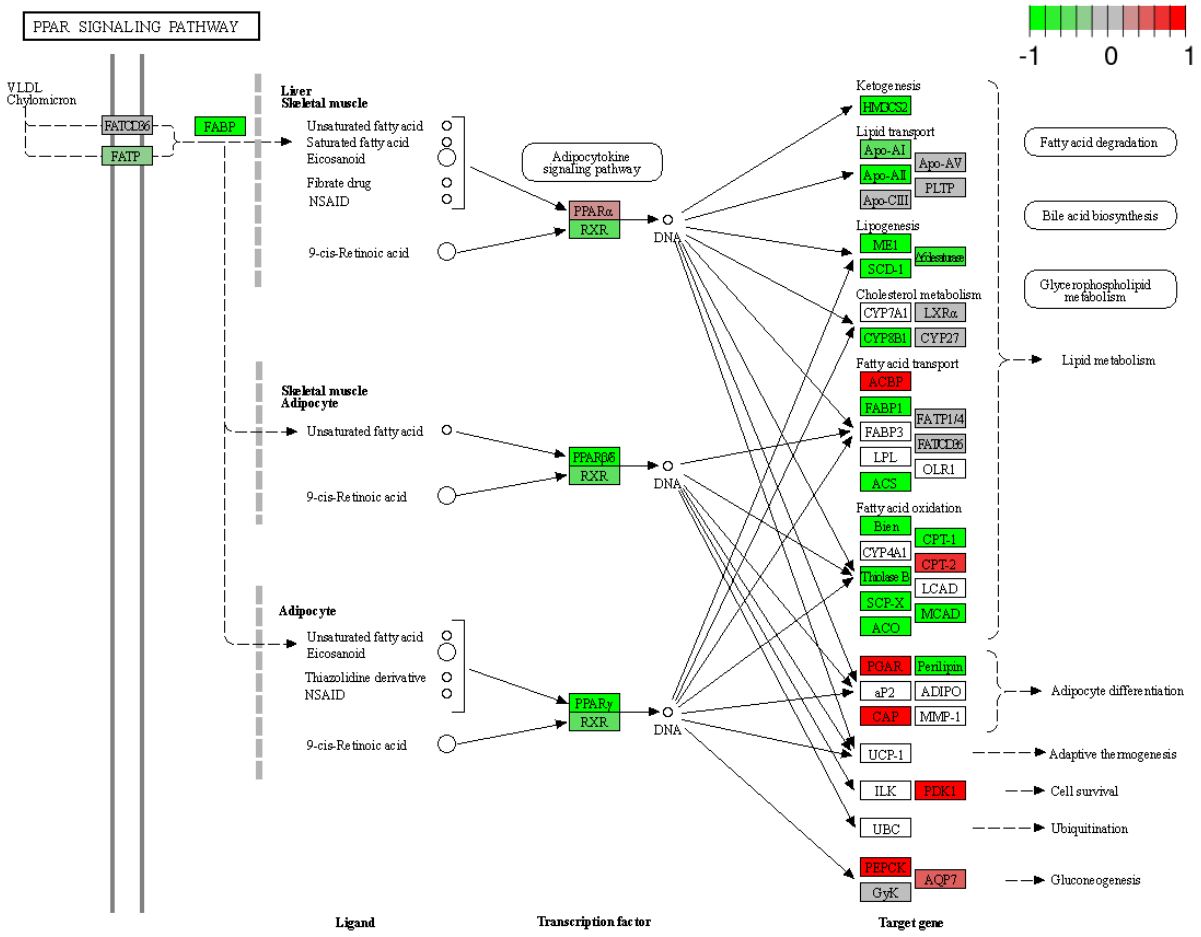

Figure S8. Effects of **2** on PPAR signaling in HepG2 cells. Colors indicate differential regulation as log2(fold change) normalized to the range -1 – 1.

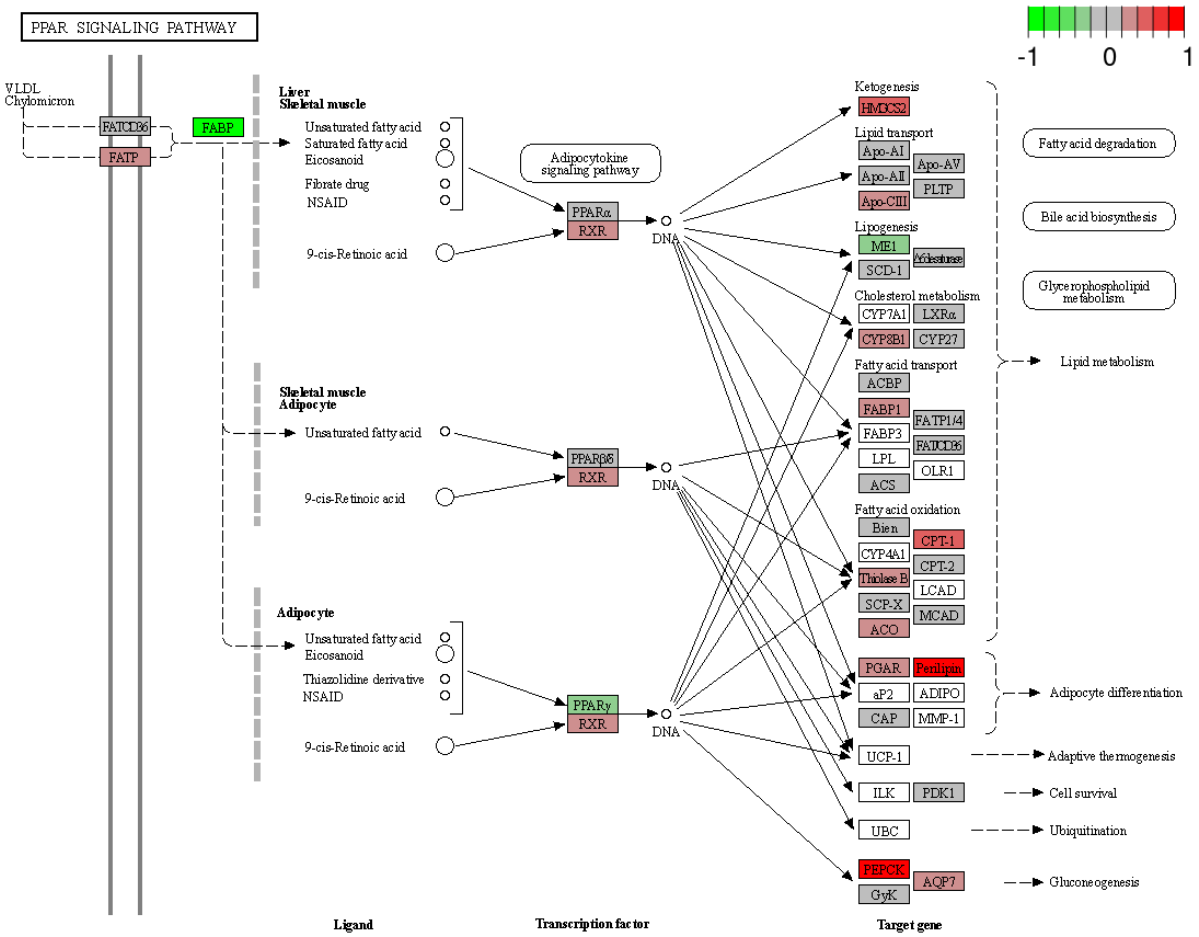

Figure S9. Effects of pioglitazone on PPAR signaling in HepG2 cells[1]. Colors indicate differential regulation as log2(fold change) normalized to the range -1 – 1.

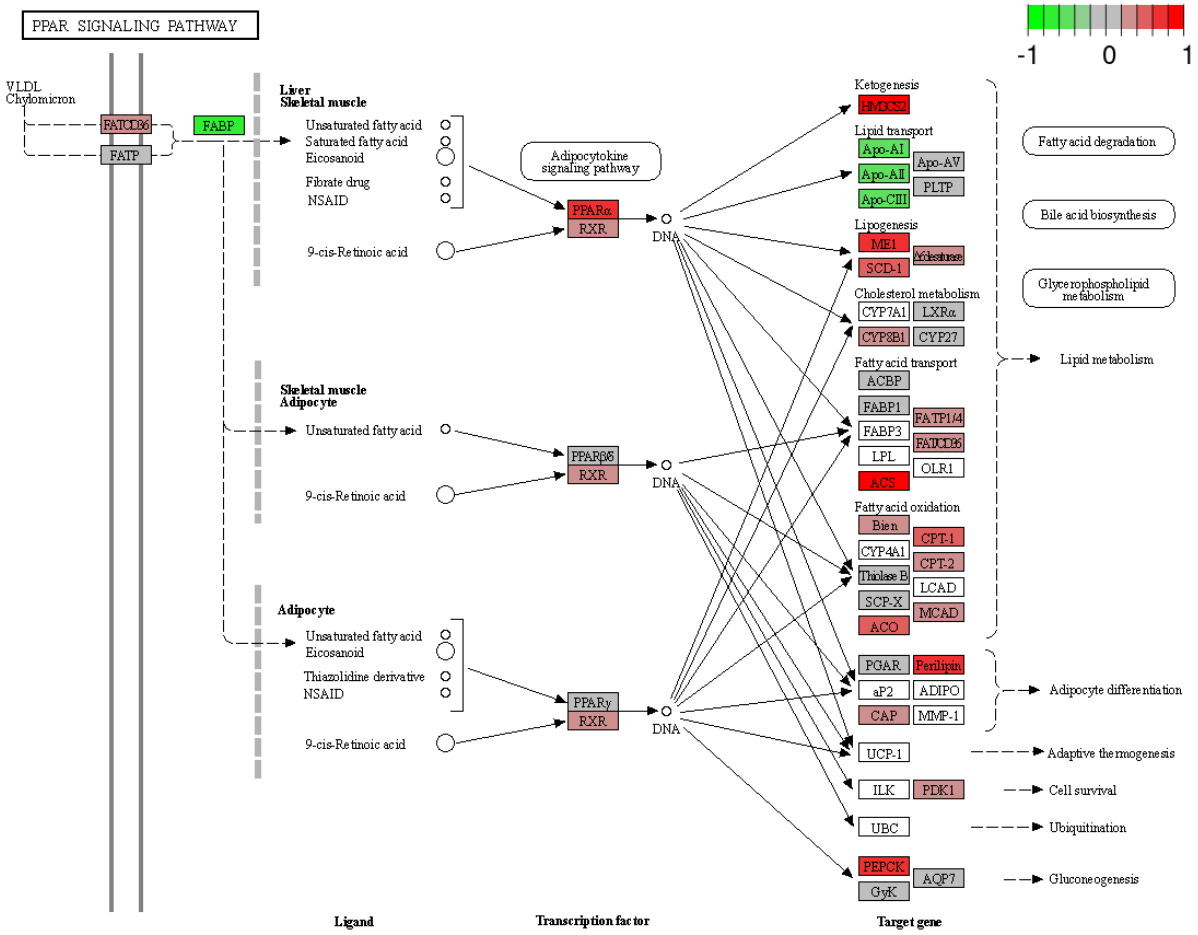

Figure S10. Effects of garcinoic acid on PPAR signaling in HepG2 cells[1]. Colors indicate differential regulation as log2(fold change) normalized to the range -1 – 1.

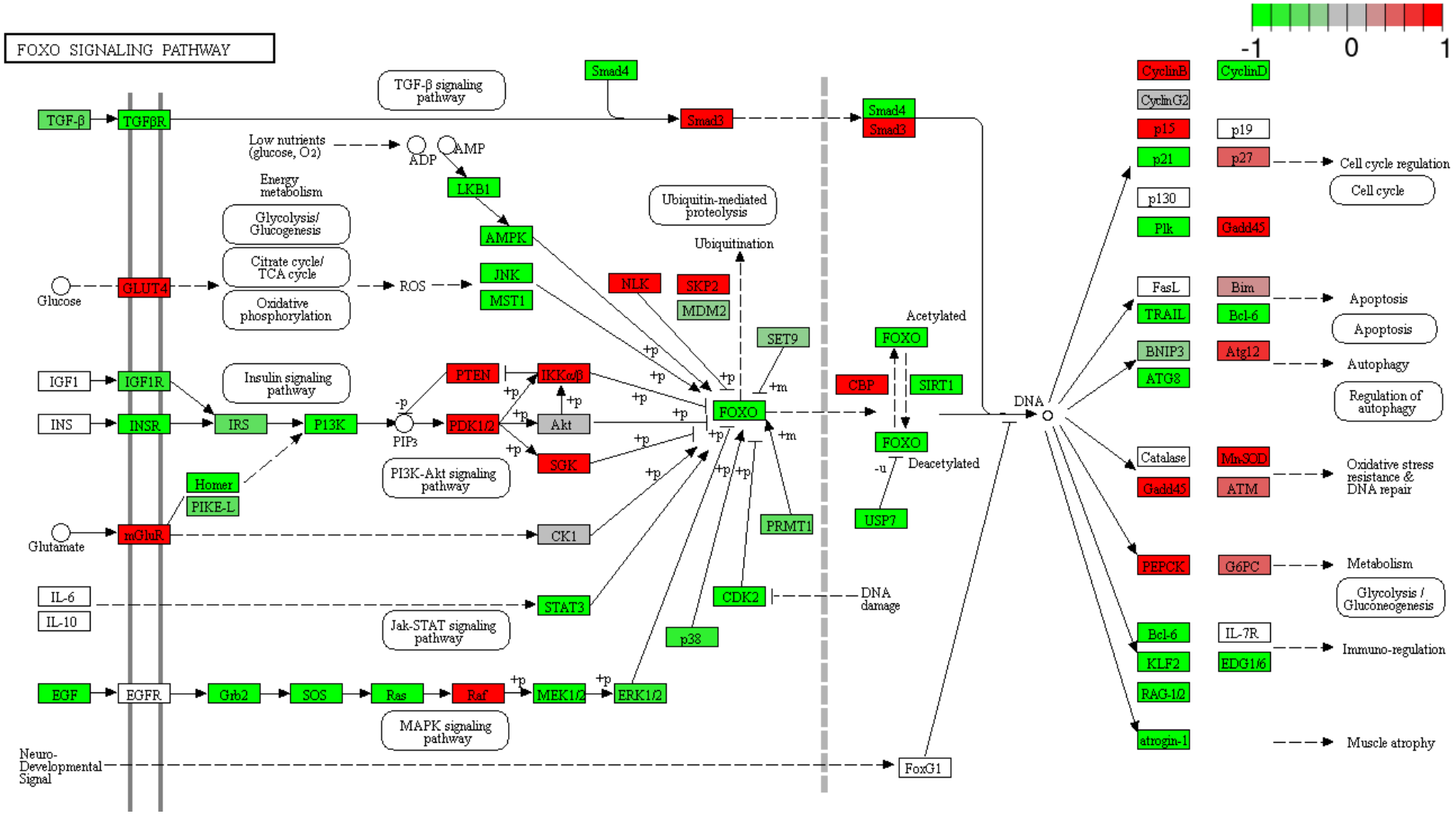

Figure S11. Effects of **2** on FOXO signaling in HepG2 cells. Colors indicate differential regulation as log2(fold change) normalized to the range -1 – 1.

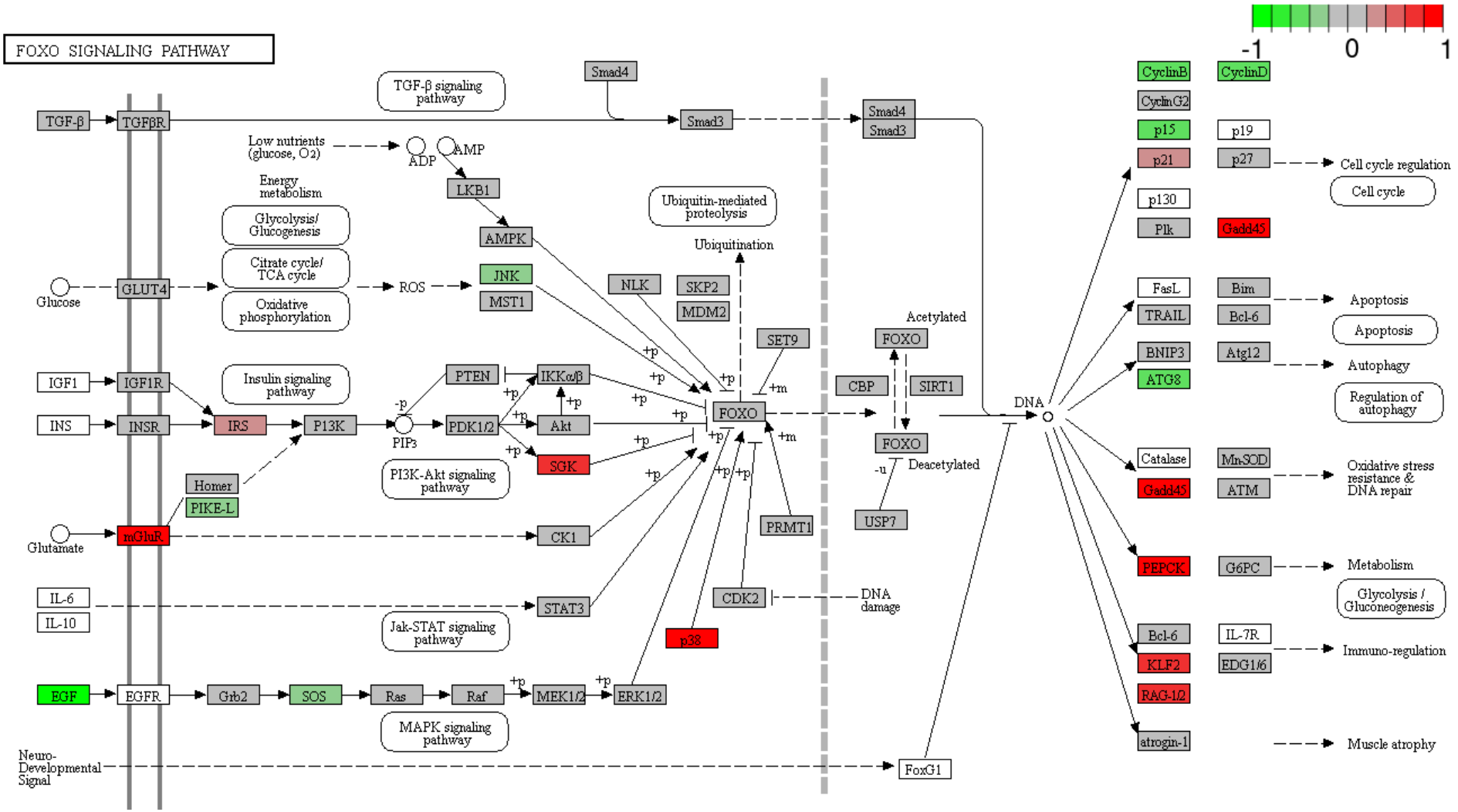

Figure S12. Effects of pioglitazone on FOXO signaling in HepG2 cells[1]. Colors indicate differential regulation as log2(fold change) normalized to the range -1 – 1.

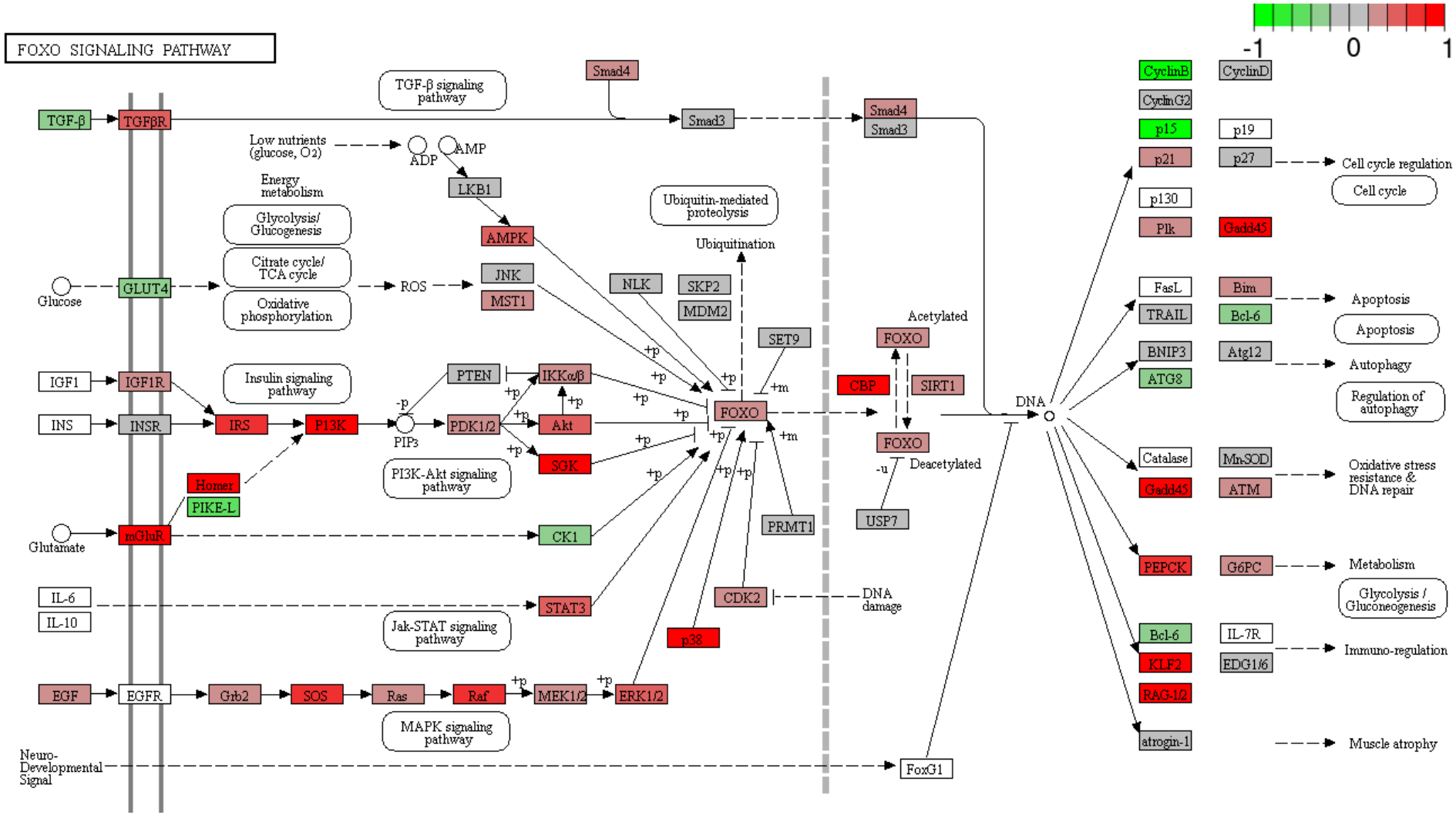

Figure S13. Effects of garcinoic acid on FOXO signaling in HepG2 cells[1]. Colors indicate differential regulation as log2(fold change) normalized to the range -1 – 1.

Table S1. Provided as supplementary file (xls) containing statistically significant (*p*-value < 0.05) effects of **2** on gene expression in HepG2 cells. Only effects with |log2(fold change)| > 1 are shown.

Table S2. Genes that were regulated by **2**, pioglitazone or GA comprising an experimentally confirmed or predicted PPAR response element. Genes are listed in alphabetical order. Data from [2].

		log2(fold_change)		
gene name	**status**	**2**	**PIO**	**GA**
A1CF	pred.			0.291
A2M	pred.	-2.312		0.661
AACS	pred.			0.241
ABCA1	pred.			0.248
ABCB10	pred.			0.544
ABCB7	pred.			0.300
ABCC1	pred.		0.191	0.362
ABCC3	pred.		0.355	0.390
ABCC4	pred.			0.682
ABCD3	pred.			0.350
ABCG2	pred.			0.582
ABCG4	pred.	-8.297		
ABHD3	pred.		0.192	0.192
ABHD5	pred.		-0.344	
ACAA2	pred.			0.235
ACACB	pred.			0.456
ACADM	pred.			0.325
ACAP3	pred.			-0.328
ACAT1	pred.			0.320
ACKR2	pred.	-7.018		
ACLY	pred.	-1.794		0.474
ACO1	pred.			0.467
ACO2	pred.			0.533
ACOT1	pred.			0.323
ACOT2	pred.		0.269	0.223
ACOX1	pred.		0.150	0.291
ACSL1	pred.			0.578
ACSL3	pred.			0.369
ACSS2	pred.			0.194
ACTB	pred.	-1.105		
ACYP2	pred.			-0.289
ADAMTSL4	pred.		0.283	0.300
ADAP2	pred.			0.486
ADCK2	pred.			0.368
ADH4	pred.			-0.367
ADIPOR2	pred.			0.382
AFAP1	pred.			0.455
AFF4	pred.			0.487
AFG3L2	pred.			0.629
AFP	pred.	-1.921		
AGL	pred.			0.332
AGPAT2	pred.		0.527	0.400
AIF1L	pred.			0.186
AK3	pred.			0.296
AKAP1	pred.			0.371
ALAS1	pred.			0.434
ALDH2	pred.			-0.305
ALDH3A1	pred.			0.530
ALDH9A1	pred.	-7.776		0.282

		log2(fold_change)		
gene name	**status**	**2**	**PIO**	**GA**
ALG9	pred.		-0.228	
ALS2	pred.			0.391
AMMECR1	pred.			0.466
AMOT	pred.			0.801
ANAPC13	pred.	-7.227		
ANGPT2	pred.			-1.618
ANKRD17	pred.			0.544
ANKRD37	pred.	4.493		
ANKRD40	pred.			0.505
ANXA5	pred.	-7.012		
ANXA6	pred.			0.216
AOC3	pred.	-7.425		
AOX1	pred.			0.799
AP1G2	pred.			-0.355
AP2A1	pred.			0.298
APEX2	pred.			0.199
APOA1	exp.	-0.495		-0.453
APOA2	pred.	-0.907		-0.457
APOC1	pred.			-0.454
APOE	pred.	-0.786		-0.312
APOE	exp.	-0.786		-0.312
APOH	pred.	-2.413		
AQP3	pred.		1.148	1.149
ARC	pred.	-8.249		
ARHGEF25	pred.			-0.283
ARHGEF40	pred.		0.216	0.187
ARID5A	pred.			-0.285
ARL2	pred.			-0.327
ARMC9	pred.			0.337
ARPP19	pred.	-7.384		0.534
ARRB1	pred.	0.771		0.432
ASGR1	pred.			-0.235
ASPDH	pred.			-0.532
ATAT1	pred.	-7.906		
ATF3	pred.			-0.381
ATF4	pred.	-1.606		
ATN1	pred.	-1.109		
ATP2A2	pred.			0.527
ATP6V0E2	pred.			0.255
ATP8B1	pred.			0.340
ATXN7L2	pred.			-0.378
AXIN2	pred.	8.523		
AZIN1	pred.			0.288
BAHD1	pred.			0.386
BANF1	pred.	-2.335		-0.463
BBX	pred.	-7.061		0.499
BCAR3	pred.	8.581		0.348
BCL2L11	pred.			0.322
BCL9	pred.			0.376

		log2(fold_change)		
gene name	status	2	PIO	GA
BDH1	pred.			-0.291
BNIP2	pred.			0.246
BRCA1	exp.			0.368
BRCA1	pred.			0.368
BRI3BP	pred.			0.394
BRPF3	pred.			0.585
BRWD1	pred.			0.229
BSG	pred.			-0.346
BTBD1	pred.			0.480
BTBD2	pred.		0.168	
BTG2	pred.			0.306
BZW2	pred.	-7.664		
C1QTNF3	pred.			-0.958
CALHM2	pred.			0.894
CALR	pred.	-4.124		
CAMK2D	pred.			0.217
CAP1	pred.			0.709
CCDC85C	pred.			1.039
CCDC92	pred.			-0.236
CCNO	pred.	-6.963		
CCT3	pred.	-1.323		
CD302	pred.			0.632
CD74	pred.			-0.381
CDA	pred.	-7.074		
CDC27	pred.	-7.083		0.268
CDC37	pred.	-0.982		-0.302
CDC45	pred.	-8.798		
CDH2	pred.	-6.892		0.449
CDH24	pred.	-1.261		
CDK2	pred.	-7.162		0.204
CDK2AP2	pred.			-0.555
CDK5	pred.	-0.421		
CDKN1A	exp.	-1.757		0.281
CDRT4	pred.			-1.594
CEBPB	pred.	-7.502		
CEBPD	pred.			-0.429
CEP170	pred.			0.313
CEP350	pred.			0.686
CERK	pred.			0.271
CHCHD10	pred.		0.291	
CHCHD3	pred.	-4.545		0.300
CHEK2	pred.	-7.583		
CHMP1A	pred.	-0.764		
CHUK	pred.			0.543
CIB1	pred.			-0.308
CISD1	pred.			0.267
CITED2	pred.			0.400
CLDN15	pred.	1.066		
CLDN5	pred.		0.548	
CLIC4	pred.			0.391
CLP1	pred.			0.384
CLSTN1	pred.			0.407
CLUH	pred.		0.244	0.403
CNKSR1	pred.			-0.311
COG4	pred.			-0.246
COL18A1	pred.	-1.258		
COL6A1	pred.			-0.282
COMMD6	pred.	-7.888		-0.334
COMTD1	pred.			-0.492
COPS6	pred.			-0.265
CORO2A	pred.			0.387
COX7B	pred.			-0.390
CPD	pred.			0.784

		log2(fold_change)		
gene name	status	2	PIO	GA
CPT1A	pred.		0.342	1.075
CPT2	pred.			0.272
CREB3L2	pred.			0.476
CREB3L3	pred.			0.435
CRY1	pred.			0.379
CS	pred.			0.248
CSF1R	pred.	-7.429		
CSNK1A1	pred.			0.985
CSRP2	pred.			-0.358
CSTB	pred.			-0.324
CUL7	pred.	-1.396		0.264
CUTA	pred.			-0.258
CWC25	pred.	-5.262		
CYGB	pred.			-0.298
CYP1A1	pred.	-6.748		1.351
CYP8B1	pred.			0.364
DAG1	pred.			0.666
DBT	pred.	0.888		0.371
DDI2	pred.			0.707
DDIT3	pred.	-8.404		-0.471
DDIT4	pred.	-7.662	0.393	0.519
DECR2	pred.			-0.300
DEDD2	pred.	-0.658		
DEGS1	pred.	-0.881		
DENND4C	pred.	1.258		0.771
DENND5A	pred.			0.253
DERL1	pred.	-7.302		
DET1	pred.	-5.432		
DGAT2	pred.			0.258
DHCR7	pred.	-1.036		0.383
DHRS3	pred.			-0.499
DIXDC1	pred.	8.722		1.139
DLAT	pred.			0.403
DLD	pred.			0.292
DLST	pred.			0.273
DNAJA2	pred.	-6.972		
DNAJC1	pred.	-7.389		
DNAJC11	pred.			0.280
DNAJC15	pred.			-0.257
DNTTIP1	pred.	-7.113		
DOCK8	pred.			0.723
DOCK9	pred.			0.943
DRD4	pred.			-1.126
DSP	pred.			0.382
DTNBP1	pred.	-8.085		
DTX4	pred.		0.512	0.747
DUSP1	pred.		0.609	
DUSP3	pred.			0.320
DYNLRB1	pred.	-0.697		-0.467
E2F8	pred.			0.386
EBPL	pred.			-0.276
ECH1	pred.	-1.343		
EEF2K	pred.			0.239
EFR3A	pred.			0.451
EHF	pred.	8.342		
EHHADH	pred.			0.342
EIF1	pred.	-1.513		-0.300
EIF4B	pred.			0.479
EIF4EBP2	pred.			0.545
ELK3	pred.	6.833		0.397
ELOVL5	pred.	-3.688		
ENAH	pred.			0.428
ENC1	pred.			-0.308

		log2(fold_change)		
gene name	status	2	PIO	GA
ENO1	pred.			0.187
EPAS1	pred.			0.575
EPHX1	pred.			0.258
EPHX2	pred.			-0.199
EPOR	pred.	-7.364		
EPS8	pred.	-8.179		0.478
ERC1	pred.			0.903
ERGIC1	pred.			0.267
ERLIN1	pred.			0.638
ERLIN2	pred.			0.275
ERMP1	pred.			0.386
ETFA	pred.			0.286
ETFDH	pred.			0.477
ETV3	pred.			0.415
ETV5	pred.			0.361
EXOC6B	pred.			0.526
EXOSC5	pred.			-0.325
EZH2	pred.			-0.212
FABP1	pred.		0.357	
FABP5	pred.			-0.291
FADS1	pred.			0.331
FADS2	pred.			0.287
FAM102A	pred.	-8.427		
FAM126A	pred.			0.337
FAM129B	pred.			0.353
FAM162A	pred.			-0.501
FAM98C	pred.			-0.316
FAR2	pred.	-6.751		
FASN	pred.	-1.217		0.400
FASTK	pred.	-0.894		-0.334
FBF1	pred.	-1.260		
FBXO21	pred.			0.356
FDPS	pred.			0.371
FGFR1	pred.			0.221
FGFRL1	pred.	-1.301	0.186	0.415
FITM2	pred.			0.641
FKBP10	pred.	-0.935		
FKBP5	pred.			0.548
FOS	pred.	-8.112		
FOSL1	pred.			-0.460
FOXN2	pred.		-0.225	
FOXN3	pred.			0.649
FOXO3	pred.	-8.046		
FRK	pred.			0.685
FRRS1	pred.			0.631
G3BP1	pred.			0.294
G6PC	pred.			0.544
GADD45GIP1	pred.			-0.369
GAL3ST1	pred.		0.314	
GAMT	pred.			-0.399
GAPDH	pred.	-1.500		
GBF1	pred.			0.417
GCC2	pred.	3.951		0.536
GCGR	pred.		1.968	
GCLC	pred.			0.243
GCLM	pred.			0.394
GEN1	pred.			-0.258
GFI1B	pred.			-1.168
GFM1	pred.			0.442
GFM2	pred.			0.347
GLDC	pred.			0.291
GLRX	pred.		-0.266	-0.313
GMFB	pred.			0.300

		log2(fold_change)		
gene name	status	2	PIO	GA
GNA11	pred.			0.374
GNA13	pred.			0.526
GNAI1	pred.	-8.514		
GNAZ	pred.			0.216
GNPNAT1	pred.			0.280
GPAM	pred.			0.361
GPC4	pred.			2.648
GPR35	pred.	-0.922		
GPRC5B	pred.	-6.837		
GPT	pred.			-0.486
GPX3	pred.		0.220	
GPX4	pred.	-0.382		-0.372
GRID2IP	pred.	-8.155		-2.893
GSTK1	pred.	0.514		-0.291
GSTM2	pred.			-0.405
GSTP1	pred.	-0.794		
GTF3A	pred.			-0.273
GTF3C4	pred.	-8.404		0.626
GUSB	pred.	-2.910		
H2AFV	pred.			-0.177
HADHA	pred.			0.377
HCFC1R1	pred.			-0.444
HDAC10	pred.	-0.771		-0.477
HDAC6	pred.			-0.197
HDHD3	pred.	0.580		
HECTD1	pred.			0.672
HECTD3	pred.	-7.780		
HES1	pred.			-0.367
HIBCH	pred.	-6.926		
HIC2	pred.	-7.252		0.305
HIPK2	pred.			0.568
HIRA	pred.	-6.682		-0.474
HMGA1	pred.			0.330
HMGCS1	pred.			0.394
HMGCS2	pred.		0.604	1.070
HMOX1	exp.		0.400	
HNRNPL	pred.	0.624		
HOMER2	pred.			0.320
HOXB7	pred.			-3.463
HOXC6	pred.	-7.152		
HPCAL1	pred.	-7.731		
HPD	pred.	0.551		
HSD17B11	pred.	-10.129		
HSD17B4	pred.			0.430
HSP90AA1	pred.			0.452
HSP90B1	pred.	-2.684		
HSPB1	pred.			-0.460
HSPD1	pred.	-2.977		
HSPE1	pred.			-0.421
HUNK	pred.			0.647
HYLS1	pred.			-0.363
IDH1	pred.	-7.375		0.290
IDH3A	pred.			0.487
IDI1	pred.			0.365
IFITM2	pred.			-0.434
IFNAR2	pred.			-0.538
IGF2	pred.			0.510
IGF2BP2	pred.	-1.349		
IL17RB	pred.			-0.432
IMPA2	pred.			0.456
IMPAD1	pred.			0.372
INA	pred.	-7.052		
INCA1	pred.			-0.356

		log2(fold_change)		
gene name	status	2	PIO	GA
INHBE	pred.			0.247
INPPL1	pred.			-0.179
IP6K1	pred.			0.433
IQSEC1	pred.			0.416
IRAK2	pred.	7.985		0.761
IRF1	exp.			-0.364
ISCA1	pred.			0.316
ISCU	pred.			-0.260
ITFG2	pred.			-0.245
ITGA6	pred.			0.574
ITPR2	pred.			0.598
IVNS1ABP	pred.			-0.213
JUND	pred.			-0.366
KAT2A	pred.			-0.342
KCTD6	pred.			-0.308
KDM2B	pred.			0.271
KDM3A	pred.			0.259
KDSR	pred.	-7.695		
KIF16B	pred.			0.354
KIF3B	pred.			0.745
KLB	pred.			0.598
KLF11	pred.			1.073
KRT18	pred.			-0.409
LACTB2	pred.			-0.277
LAMB1	pred.			0.278
LAMB2	pred.			0.179
LAMC3	pred.			0.499
LBR	pred.			0.345
LCAT	pred.			-0.481
LDLR	pred.			0.727
LETM1	pred.			0.214
LGALS1	pred.			-0.298
LIN28B	pred.			0.606
LIPA	exp.			0.497
LIPG	pred.			0.400
LMAN1	pred.	-7.827		0.454
LNX2	pred.			0.355
LONP1	pred.		0.217	0.196
LPCAT3	pred.			1.091
LPIN1	pred.			0.343
LPIN2	pred.			0.505
LRIG3	pred.			0.737
LRP1	exp.			0.947
LRP11	pred.			0.365
LRP4	pred.			0.494
LRPPRC	pred.			0.458
LRRC59	pred.	-2.217		
LRRC8A	pred.	-6.896		0.220
LRRC8B	pred.			0.375
LSS	pred.			0.339
LTBP3	pred.			-0.192
LYSMD3	pred.			0.374
MACF1	pred.			0.616
MAF1	pred.	-1.196		
MAFG	pred.			0.400
MAP3K2	pred.			0.274
MAP4K3	pred.			0.489
MAZ	pred.			0.380
MBD2	pred.			-0.348
MBNL3	pred.			0.437
MBOAT7	pred.			0.239
MCF2L	pred.			-0.245
MCM7	pred.			0.316

		log2(fold_change)		
gene name	status	2	PIO	GA
MCM8	pred.			0.364
MEF2D	pred.			0.237
MEGF9	pred.			0.553
MERTK	pred.			0.366
METTL5	pred.			-0.268
MGAT1	pred.			0.241
MGAT4B	pred.		0.166	0.208
MGST2	pred.			-0.336
MGST3	pred.	-2.101		
MIPEP	pred.			0.335
MKI67	pred.			0.554
MLYCD	pred.	-7.431		0.355
MPRIP	pred.			0.322
MRPL18	pred.			-0.364
MRPL23	pred.	-1.078		-0.712
MRPL37	pred.			0.208
MRPL47	pred.			-0.309
MRPL54	pred.			-0.345
MRPL9	pred.	-7.206		
MRVI1	pred.	7.160		
MSLN	pred.			-0.354
MTHFD1	pred.			0.295
MTHFD2	pred.			0.376
MTOR	pred.			0.336
MUL1	pred.			0.543
MUS81	pred.			-0.385
MYC	pred.			0.416
MYH14	pred.			0.436
MYH3	pred.			-0.420
MYO18A	pred.			0.340
MYO1C	pred.			0.266
MYOM3	pred.			0.392
NAA10	pred.	-0.411		-0.453
NAA50	pred.			0.437
NAMPT	exp.			0.391
NCAPD3	pred.			0.240
NCEH1	pred.	7.985		0.383
NCOR2	pred.			0.368
NCS1	pred.			0.340
NDRG1	pred.		0.281	0.584
NDUFA11	pred.			-0.385
NDUFA5	pred.			-0.283
NDUFA6	pred.			-0.306
NDUFA8	pred.	-1.252		-0.303
NDUFA9	pred.	-2.346		-0.599
NDUFAF3	pred.			-0.506
NDUFB10	pred.			-0.318
NDUFB8	pred.	-1.244		
NDUFS1	pred.	0.833		0.428
NDUFS2	pred.			0.298
NDUFS8	pred.			-0.284
NDUFV3	pred.			-0.312
NEIL1	pred.			-0.283
NEK9	pred.			0.236
NEURL4	pred.	-0.882		
NFATC4	pred.	-0.488		
NFE2	pred.		0.335	
NFE2L1	pred.			0.524
NFIX	pred.	-9.205		
NFKB2	pred.			-0.293
NGFR	pred.	-7.456	0.715	
NLN	pred.			0.416
NME7	pred.	8.007		

		log2(fold_change)		
gene name	status	2	PIO	GA
NMNAT1	pred.			0.255
NMT2	pred.			0.276
NNAT	pred.			0.559
NPC1	pred.			0.464
NPEPL1	pred.			-0.349
NPR3	pred.	7.306		
NQO1	pred.			0.218
NR2C1	pred.			-0.349
NR2F6	pred.	-0.942		
NRCAM	pred.	-7.862		
NT5C2	pred.	8.341		0.455
NT5E	pred.		-0.338	
NUCB2	pred.			-0.287
NUDT14	pred.			-0.368
NUPL2	pred.		-0.220	
NUS1	pred.			0.253
NXPH3	pred.		0.710	0.693
OAS3	pred.			0.331
OGFOD3	pred.			0.198
OPHN1	pred.			0.633
OSBPL11	pred.	-6.831		0.371
OSR1	pred.			-0.584
OXR1	pred.			0.542
PABPN1	pred.			-0.350
PACS1	pred.	1.121		0.260
PAK2	pred.			0.379
PAN2	pred.			-0.354
PARP11	pred.			0.489
PARP14	pred.		-0.235	
PASK	pred.			0.191
PCK1	pred.		0.775	0.667
PCSK4	pred.			-0.362
PCSK5	pred.			0.570
PCSK6	pred.	0.945		0.829
PCSK7	pred.			0.492
PCTP	pred.			0.494
PDK2	pred.			0.234
PDLIM5	pred.			0.400
PDP2	pred.			0.351
PDRG1	pred.	-2.779		
PDZK1	pred.		0.202	
PELI3	pred.			0.284
PEX11A	pred.		0.255	0.373
PEX19	pred.			0.277
PEX5	pred.			0.491
PFKFB3	pred.	-7.081		0.577
PFKL	pred.		0.199	
PGD	pred.	-1.019		
PGS1	pred.		0.178	
PHB2	pred.	-0.807		
PHLPP2	pred.			0.456
PIAS1	pred.			0.293
PIK3IP1	pred.	8.121		
PIM1	pred.		0.242	
PIP5K1A	pred.			0.203
PIP5K1B	pred.			0.376
PJA1	pred.	-6.916		0.448
PKDCC	pred.			-0.270
PKP2	pred.			0.313
PLEKHH1	pred.	-7.421		
PLEKHM2	pred.			0.189
PLIN2	exp.		0.649	0.978
PLIN4	pred.		0.419	

		log2(fold_change)		
gene name	status	2	PIO	GA
PLIN5	pred.			-0.410
PLK3	pred.			-0.370
PLXNA2	pred.			0.252
PMPCB	pred.	1.235		
PNN	pred.			-0.303
PNPLA1	pred.	-7.237		
PNPLA3	pred.			0.671
POLR2A	pred.			0.616
POLR2F	pred.	-1.195		-0.349
POP5	pred.			-0.402
POR	pred.		0.207	0.298
PPARA	pred.			0.792
PPIF	pred.			0.207
PPM1F	pred.			0.264
PPM1L	pred.			0.335
PPP1CC	pred.	-8.439		
PPP1R14B	pred.	-1.133		
PPP1R15B	pred.			0.418
PPP2R5B	pred.			-0.467
PPP3CA	pred.			0.345
PRADC1	pred.			-0.357
PRDX6	pred.			-0.220
PREPL	pred.			0.371
PRKAR2A	pred.			0.608
PRKCA	pred.			0.827
PRKDC	pred.			0.962
PRKRIP1	pred.			-0.280
PROSER2	pred.	-8.287		
PROX1	pred.	-6.988		0.327
PRPS1	pred.			0.357
PRR36	pred.			-0.447
PRSS8	pred.			0.374
PSMA1	pred.			-0.385
PSMD7	pred.			1.064
PSME2	pred.	-8.272		-0.296
PSRC1	pred.			-0.326
PTGES	pred.	-7.034		
PTGR1	pred.	-7.193		0.711
PTPN6	pred.			-0.367
PUS7L	pred.			0.313
PYROXD2	pred.			-0.398
PZP	pred.	8.362		
RAB11FIP4	pred.			0.279
RAB11FIP5	pred.		0.353	0.595
RAB3D	pred.			0.546
RAD21	pred.	8.089		
RAD23B	pred.	-6.655		
RAD54L	pred.			0.182
RALGAPA2	pred.			0.968
RAP1GAP2	pred.			0.431
RARB	pred.	7.219		
RARRES2	pred.			-0.306
RASD1	pred.	-6.855		-0.449
RASIP1	pred.	-5.111		
RASL10B	pred.			0.607
RASSF3	pred.			0.325
RASSF4	pred.			-0.317
RBKS	pred.	-7.850		
RBM39	pred.			-0.451
RBP1	pred.			-0.456
RBPMS	pred.			-0.271
RBX1	pred.			-0.423
RCL1	pred.	-8.739		

		log2(fold_change)		
gene name	status	2	PIO	GA
RCN1	pred.			-0.264
RCN3	pred.			-0.581
REEP6	pred.			-0.275
RETSAT	pred.		0.187	0.264
REV3L	pred.			0.660
RGL3	pred.			-0.321
RGP1	pred.			0.665
RGS3	pred.	-8.830	0.255	0.353
RHBDF1	pred.			-0.379
RHOG	pred.			-0.336
RHPN2	pred.			0.348
RMND1	pred.	0.535		
RNF111	pred.			0.482
RNF144A	pred.			0.589
RNF168	pred.			0.217
RNF34	pred.	-7.423		
RNF7	pred.			-0.445
ROCK2	pred.			0.447
RPL14	pred.	-1.414		-0.361
RPL3	pred.	-0.822		
RPP30	pred.			-0.232
RPRD1B	pred.			0.501
RPTOR	pred.			0.243
RRBP1	pred.	-0.752		-0.205
RRN3	pred.			0.215
RRP1B	pred.			0.314
RUNDC1	pred.			0.253
S100A1	pred.			-0.472
S100A10	pred.	-7.730		-0.334
S100A13	pred.			-0.396
SAT1	exp.			-0.291
SC5D	pred.			0.333
SCAMP5	pred.			0.403
SCARB1	exp.			0.199
SCARB2	pred.			0.457
SCN4B	pred.		2.141	
SCO1	pred.			0.322
SCRN1	pred.			0.524
SCYL2	pred.			0.354
SDC4	pred.			0.275
SDCBP2	pred.	7.966		
SDHA	pred.			0.186
SDHB	pred.	-7.353		
SEC23A	pred.			0.628
SEL1L	pred.			0.752
SEL1L3	pred.			0.726
SEMA3G	pred.			0.307
SEMA4B	pred.			0.325
SENP3	pred.	-2.746		0.296
SERPINE1	pred.			0.316
SERPINF1	pred.	-0.998		
SERPINI1	pred.	-7.710		
SF3B4	pred.	-1.633		
SFSWAP	pred.			-0.284
SGK1	exp.	6.827	0.204	
SGK2	pred.		0.607	0.787
SGTB	pred.		-0.348	
SH3BGRL2	pred.			0.378
SH3BP2	pred.	0.692		0.194
SHANK3	pred.			0.388
SIAH2	pred.			0.218
SLC16A1	pred.			0.493
SLC1A5	pred.	-0.916		

		log2(fold_change)		
gene name	status	2	PIO	GA
SLC25A20	pred.			0.657
SLC25A42	pred.		0.376	0.426
SLC25A44	pred.			0.237
SLC25A47	pred.		0.646	
SLC25A5	pred.			0.257
SLC27A4	pred.			0.323
SLC29A3	pred.	-7.547		0.467
SLC2A4	pred.			-0.332
SLC31A1	pred.			0.671
SLC38A4	pred.			0.623
SLC41A1	pred.			0.479
SLC44A1	pred.			0.243
SLC48A1	pred.			0.330
SLC4A2	pred.			0.430
SLC4A7	pred.			0.559
SLC52A2	pred.	-1.005		
SLC6A8	pred.		0.230	
SLC8A3	pred.	-7.470		
SLIT2	pred.	-6.892		
SMAD5	pred.			0.445
SMAD7	pred.	-7.571		
SMAP2	pred.			0.340
SMARCA2	pred.			0.438
SMARCA4	pred.			0.270
SMARCA5	pred.	-8.361		0.259
SMPD3	pred.	-6.813		-0.618
SNN	pred.	-6.813		0.211
SNRNP70	pred.	-1.851		-0.249
SNRPB	pred.	-0.668		
SNX6	pred.			0.316
SOD1	pred.			-0.297
SOD2	pred.	1.640		
SOGA1	pred.			0.488
SORD	pred.	-6.903		0.357
SOX13	pred.			0.236
SOX9	pred.	4.442		
SPATC1	pred.			1.314
SPC25	pred.	1.089		
SPIRE2	pred.			-0.238
SPNS1	pred.	-7.425		
SPNS2	pred.		0.928	
SPSB1	pred.	-8.263		
SQSTM1	pred.			0.601
SRP68	pred.			0.271
SRP72	pred.			0.382
SRPX2	pred.			-0.462
SRSF6	pred.			-0.396
SSH2	pred.			0.464
ST3GAL6	pred.			-0.531
ST6GALNAC4	pred.			0.335
STARD10	pred.			-0.434
STAT1	pred.			0.477
STAT5A	pred.			0.564
STBD1	pred.	-8.913		
STIM1	pred.	-7.269		0.400
STK10	pred.			0.357
STK38L	pred.			0.358
STOML2	pred.	-1.717		
STX18	pred.			-0.229
SUCLG2	pred.			0.283
SUDS3	pred.			0.347
SULF2	pred.	-6.676		
SULT2A1	pred.		0.192	0.296

		log2(fold_change)		
gene name	status	2	PIO	GA
SYNJ2	pred.			0.203
TAF9	pred.	-7.001		
TAF9B	pred.	1.668		
TAGLN2	pred.	-1.275		
TAZ	pred.			-0.335
TBC1D8	pred.			-0.199
TBX10	pred.			-0.595
TCEA3	pred.			-0.263
TECR	pred.			-0.311
TEX2	pred.			0.346
TFB1M	pred.			-0.321
TFPI	pred.		-0.245	-0.296
TGFA	pred.			0.330
TGFBI	pred.			0.299
TGFBR2	pred.	-6.822		0.472
TGM2	pred.			0.428
THOC6	pred.			-0.343
THOP1	pred.	-0.917		
TIMM23	pred.	-9.876		
TIMM8B	pred.			-0.285
TIMM9	pred.			-0.284
TIMP1	pred.			-0.505
TLCD1	pred.	-1.409		
TLE3	pred.	-0.798		
TM7SF2	pred.	-0.935		
TMBIM1	pred.			0.208
TMCO6	pred.			-0.261
TMED8	pred.			0.424
TMEM11	pred.			-0.305
TMEM135	pred.			0.329
TMEM136	pred.			0.344
TMEM164	pred.			0.488
TMEM170B	pred.			0.371
TMEM25	pred.	-8.038		
TMEM37	pred.			0.174
TMEM53	pred.		0.329	0.318
TMEM63B	pred.		0.162	0.159
TMEM64	pred.			0.518
TMTC1	pred.			0.733
TNFRSF12A	pred.			-0.472
TNFSF10	exp.	-7.627		
TNFSF12	pred.	-7.062		-0.311
TNIP1	exp.	-1.395		
TNNC1	pred.	0.676		
TOR1B	pred.			0.358
TOR3A	pred.			0.304
TPD52L1	pred.	3.029		
TPM2	pred.			-0.706
TRIM14	pred.	7.939		0.463
TRIM25	pred.			0.530
TRIM35	pred.			0.387
TRIM44	pred.			0.588
TRIO	pred.			0.393
TRIT1	pred.			-0.317
TRPT1	pred.			-0.378
TRPV1	pred.			-0.337
TRUB1	pred.			0.505
TSC22D1	exp.			0.207
TSKU	pred.			0.329
TSPAN17	pred.			0.282
TSPO	pred.	-3.315		
TTC39B	pred.	1.154		
TTF2	pred.			0.301

		log2(fold_change)		
gene name	status	2	PIO	GA
TTI1	pred.			0.418
TUBA4A	pred.			-0.418
TUFM	pred.	-0.788		
TYSND1	pred.		0.245	
UBAP1	pred.			0.204
UBE2C	pred.			-0.362
UBE4B	pred.			0.315
UBFD1	pred.			0.408
UBQLN1	pred.	-1.527		0.418
UBXN11	pred.			-0.412
UBXN2B	pred.			0.374
UCKL1	pred.			-0.248
UFM1	pred.	-6.821		
UGDH	pred.			0.490
UQCR10	pred.	-1.586		-0.452
UQCRQ	pred.	-1.431		-0.376
URGCP	pred.			-0.294
UROD	pred.	-0.610		
USP6NL	pred.			0.250
USP8	pred.			0.462
VAPB	pred.	-4.017		0.306
VAT1	pred.			0.240
VEGFA	exp.			-0.274
VNN1	pred.	8.703		
VRK2	pred.			0.545
WAC	pred.			0.303
WARS	pred.			0.312
WBP11	pred.			0.205
WDR1	pred.			0.288
WDR48	pred.			0.538
WDR6	pred.	-8.480		
WDR76	pred.			0.408
WWTR1	pred.			0.294
XIAP	pred.			0.382
XIRP2	pred.	7.002		
XRCC5	pred.	-1.299		0.194
YARS	pred.			0.285
YIF1A	pred.	-0.985		
YPEL3	pred.			-0.546
YWHAB	pred.			0.293
ZC3H3	pred.			-0.309
ZDHHC12	pred.			-0.410
ZDHHC8	pred.			-0.285
ZHX2	pred.	-8.141		0.419
ZMYND15	pred.			-0.620
ZNHIT1	pred.	0.593		-0.459
ZNHIT6	pred.			0.256

Synthesis of 2

2 was synthesized over seven convergent steps following previously reported protocols[3,4] with adaptions according to Scheme S1. Thiobarbituric acid (**3**) was reacted with ethyl bromoacetate (**4**) to thioether **5** which was then chlorinated using $POCl_3$ to obtain **6**. In parallel, 3-nitrophenol (**7**) was methylated with iodomethane to **8** and subsequently hydrogenated to aniline **9**. Aniline **9** and chloropyrimidine **6** were then coupled to **10** by nucleophilic aromatic substitution. After demethylation of the methoxy group and concomitant ester hydrolysis with boron tribromide to **11**, Williamson ether synthesis with 2-bromoethylbenzene (**12**) produced **2** in 12% overall yield.

Scheme S1. Synthesis of **2**.[a]

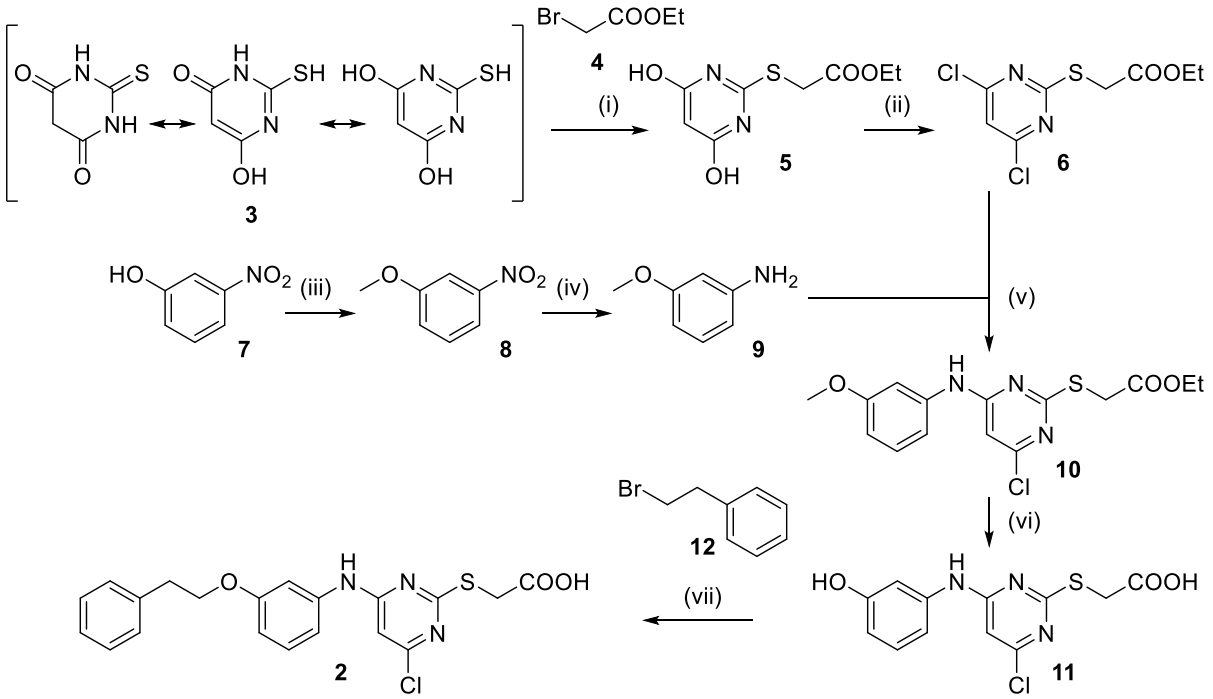

[a] Reagents & Conditions: (i) NaOH, H_2O/EtOH, 60 °C, 4.5 h, 65%; (ii) $POCl_3$, diethyl aniline, 90 °C, 5 h, 75%; (iii) CH_3I, NaH, DMF, r.t., 24 h, 82%; (iv) H_2, Pd(C), EtOAc, r.t., 15 h, 92%; (v) Hünig's base, DMF, 120 °C, 20 h, 63%; (vi) BBr_3, CH_2Cl_2, r.t., 16 h, 81%; (vii) K_2CO_3, KI, DMF, 80 °C, 23 h, 47%.

Materials & Methods

Chemistry

General

All chemicals and solvents used were obtained from commercial sources (Sigma Aldrich, TCI, Alfa Aesar, BLDpharm). They were at least 95% pure and were used without further purification. Reactions were performed when needed with argon as an inert gas in absolute solvents from Sigma Aldrich. For purification by column chromatography, technical solvents, without further purification, were used. The deuterated solvents DMSO-d_6 and MeOH-d_4 used for NMR spectroscopy were purchased and used without further drying. Reactions were monitored by thin-layer chromatography (TLC) using silica gel (particle size of 60 µM) coated aluminum plates with UV254 fluorescence indicator from Macherey-Nagel. Purification by column chromatography was performed using silica gel from Sigma Aldrich. NMR spectra were recorded on a Bruker AV 500 spectrometer (Bruker Corporation, Billerica, MA, USA). Chemical shift (δ) values were expressed in ppm and coupling constants (*J*) in hertz (Hz). ESI mass spectra were recorded on a VG Platform II instrument (Thermo Fisher Scientific, Waltham, MA, USA) and high-resolution mass spectra on an LTQ Orbitrap XL instrument (Thermos Fisher Scientific). Purity of all final products was analyzed by HPLC on a Varian ProStar HPLC from SpectraLab Scientific Inc. equipped with a MultiHigh 100 Phenyl-5µ, 240 + 4 mm column, at a flow rate of 1 mL per minute and UV detection (254 nm and 280 nm). Only compounds with a purity of ≥ 95% (AUC at 254 nm and 280 nm) were used for biological assays. The synthesis of **1** and precursors has been reported previously[4].

Synthesis and analytical characterization data

3-Nitroanisole (**8**): DMF (15 mL) was added to 3-nitrophenol (**7**, 642 mg, 4.61 mmol, 1.00 eq) and NaH (111 mg, 4.61 mmol, 1.00 eq) at 0 °C. Methyl iodide (315 µL, 5.07 mmol, 1.10 eq) was added dropwise at 0 °C and the reaction mixture was stirred at room temperature for 24 hours. Then H_2O (10 mL) was added, and the mixture was extracted three times with ethyl acetate (10 mL). The organic layers were combined, dried over Na_2SO_4 and the solvent was evaporated in vacuo. Further purification was performed by column chromatography (*n*-hexane/ethyl acetate 9:1) to yield **8** as a colorless solid (82%). ^{1}H-NMR (300 MHz, methanol-d_4): δ = 7.78-7.74 (m, 1H), 7.68-7.67 (m, 1H), 7.46 (t, *J* = 8.2 Hz, 1H), 7.30-7.26 (m, 1H), 3.86 (s, 3H) ppm. ^{13}C-NMR (75 MHz, methanol-d_4): δ = 160.34, 129.91, 120.54, 115.03, 107.94, 55.01 ppm. MS (ESI+): *m/z* no molecular ion.

***m*-Anisidine** (**9**): 3-Nitroansiole (**8**, 1.21 g, 7.89 mmol, 1.00 eq) was dissolved in ethyl acetate (100 mL) and Pd(C) (84.0 mg, 789 µmol, 0.10 eq) was added. The suspension was stirred at room temperature under hydrogen atmosphere for 15 hours. The reaction mixture was then filtered through Celite and dried over Na_2SO_4. Evaporation of the solvent in vacuo yielded **9** as a brown oil (92%). ^{1}H-NMR (300 MHz, DMSO-d_6): δ = 6.89 (t, *J* = 8.1 Hz, 1H), 6.16-6.13 (m, 2H), 6.09-6.05 (m, 1H), 5.01 (s, 2H), 3.64 (s, 3H) ppm. ^{13}C-NMR (75 MHz, DMSO-d_6): δ = 160.27, 149.98, 129.54, 106.86, 101.47, 99.44, 55.54 ppm. MS (ESI+): *m/z* 124.06 ([M+H]$^+$).

Ethyl 2-((4-chloro-6-((3-methoxyphenyl)amino)pyrimidin-2-yl)sulfanyl)acetate (**10**): Ethyl-2-((4,6-dichloropyrimidin-2-yl)sulfanyl)acetate (**6**, 256 mg, 957 µmol, 1.00 eq) was dissolved in a mixture of DMF (10 mL) and diisopropylethylamine (157 µL, 1.14 mmol, 1.19 eq). m-Anisidine (**9**, 118 mg, 957 µmol, 1.00 eq) was added, and the solution was stirred for 20 h at 120 °C. After cooling to room temperature, ethyl acetate (30 mL) was added, and the mixture was washed three times with H_2O (30 mL). The organic layer was dried over Na_2SO_4 and the solvent was evaporated in vacuo. Further purification was performed by column chromatography (*n*-hexane/acetone 8:1) to yield **10** as a brown oil (63%). ^{1}H-NMR (300 MHz, methanol-d_4): δ = 7.23 (t, *J* = 8.1 Hz, 1H), 7.17-7.16 (m, 1H), 7.09-7.05 (m, 1H), 6.71-6.67 (m, 1H), 6.43 (s, 1H), 4.11 (q, *J* = 7.1 Hz, 2H), 3.96 (s, 2H), 3.01 (s, 3H), 1,20 (t, *J* = 7.1 Hz, 3H) ppm. ^{13}C-NMR (75 MHz, methanol-d_4): δ = 170.53, 169.64, 161.13, 160.29, 158.21, 139.63, 129.27, 113.15, 109.2, 106.77, 100.29, 61.35, 54.39, 32.66, 12.99 ppm. MS (ESI+): *m/z* 375.99 ($[M+Na]^+$).

2-((4-Chloro-6-((3-hydroxyphenyl)amino)pyrimidin-2-yl)sulfanyl)acetic acid (**11**): Ethyl 2-((4-chloro-6-((3-methoxyphenyl)amino)pyrimidin-2-yl)sulfanyl)acetate (**10**, 212 mg, 599 µmol, 1.00 eq) was dissolved in dichloromethane (7 mL). Boron tribromide (115 µL, 1.20 mmol, 2.00 eq) was added dropwise and the reaction was stirred at room temperature for 16 hours. Then H_2O (10 mL) was added and the mixture was extracted three times with ethyl acetate (10 mL). The organic layers were combined, dried over Na_2SO_4 and the solvent was evaporated in vacuo. Further purification was performed by column chromatography (*n*-hexane/acetone 3:2) to yield **11** as a beige solid (81%). ^{1}H-NMR (300 MHz, methanol-d_4): δ = 7.14 (t, *J* = 8.4 Hz, 1H), 7.01-6.98 (m, 2H), 6.57-6.53 (m, 1H), 6.41 (s, 1H), 3.95 (s, 2H) ppm. ^{13}C-NMR (75 MHz, methanol-d_4): δ = 171.5, 170.6, 161.2, 158.2, 157.7, 139.5, 129.4, 112.3, 110.9, 107.95, 99.9, 32.7 ppm. MS (ESI+): *m/z* 312.08 ($[M+H]^+$).

2-((4-Chloro-6-((3-phenethoxyphenyl)amino)pyrimidin-2-yl)thio)acetic acid (**2**): 2-((4-Chloro-6-((3-hydroxyphenyl)amino)pyrimidin-2-yl)sulfanyl)acetic acid (**11**, 42.2 mg, 136 µmol, 1.00 eq), 2-bromoethylbenzene (**12**, 18.5 µL, 136 µmol, 1.00 eq) and K_2CO_3 (56.3 mg, 407 µmol, 2.99 eq) were suspended in DMF (10 mL) and the mixture was stirred at 80 °C for 27 hours. After cooling to room temperature, ethyl acetate was added, and the mixture was washed three times with H_2O (30 mL). The organic layer was dried over Na_2SO_4 and the solvent was evaporated in vacuo. Further purification was performed by column chromatography (*n*-hexane/acetone 2:1) to yield **2** as a beige oil (47%). ^{1}H-NMR (500 MHz, methanol-d_4): δ = 7.22-7.19 (m, 2H), 7.15-7.14 (m, 3H), 7.11 (t, *J* = 8.1 Hz, 1H), 7.01-7.00 (m, 1H), 6.93-6.91 (m, 1H), 6.58-6.56 (m, 1H), 6.37 (s, 1H), 4.23 (t, *J* = 6.9 Hz, 2H), 3.92 (s, 2H), 2.85 (t, *J* = 6.9 Hz, 2H) ppm. ^{13}C-NMR (125 MHz, methanol-d_4): δ = 171.75, 171.08, 162.47, 159.48, 159.05, 140.81, 139.15, 130.70, 129.87, 129.38, 127.41, 113.62, 112.25, 109.46, 101.49, 67.35, 35.77, 33.98 ppm. MS (ESI+): *m/z* 438.50 ($[M+Na]^+$). HRMS (MALDI): *m/z* calculated 416.08302 for $C_{20}H_{18}ClN_3O_3S$, found 416.08310 ($[M+H]^+$).

PPARγ LBD expression, purification and crystallization

The recombinant PPARγ LBD was expressed in *E. coli* and purified initially by Ni^{2+}-affinity chromatography. The N-terminal histidine tag was removed by TEV treatment, and the cleaved protein was further purified by size exclusion chromatography in 20 mM Tris, pH 7.5, 200 mM NaCl, 0.5 mM TCEP. The ligands (4 mM; ~10-fold excess) were added to the protein (13 mg/mL) prior to crystallization using sitting drop vapour diffusion at 20 °C and the conditions listed in table below. Crystals were cryo-protected with mother liquor supplemented with 25% glycerol or 20% ethylene glycol. Diffraction data were collected at Swiss Light Source, and were processed and scaled with XDS[5] and aimless[6], respectively. Molecular replacement was performed using Phaser[7] and the coordinates of PPARγ (pdb id 6TSG[8]). Manual model rebuilding alternated with structure refinement were performed in COOT[9] and REFMAC5[10]. The data collection and refinement statistics are summarized in the table below.

Data collection and refinement statistics

Complex	**1** (JP85)	**2** (SA112)	**WY14643** (dual binding; active form)	**WY14643** (single binding; inactive form)	Apo inactive
PDB accession code	8ATY	8ATZ	8CPI	8CPH	8CPJ
Data Collection					
Resolution[a] (Å)	44.30-1.90 (1.97-1.90)	46.33-1.95 (2.02-1.95)	46.38-2.10 (2.17-2.10)	44.50-2.40 (2.51-2.40)	44.62-2.40 (2.48-2.40)
Spacegroup	$P\,4_32_12$	$P\,4_32_12$	$P\,4_32_12$	$P\,2_12_12_1$	$P\,4_12_12$
Cell dimensions	*a, b* = 65.3, *c* = 156.0 Å *α, β, γ* = 90.0°	*a, b* = 65.5, *c* = 157.4 Å *α, β, γ* = 90.0°	*a, b* = 65.6, *c* = 157.3 Å *α, β, γ* = 90.0°	*a* = 62.5, *b* = 63.4, *c* = 168.4 Å *α, β, γ* = 90.0°	*a, b* = 63.1, *c* = 168.1 Å *α, β, γ* = 90.0°
No. unique reflections[a]	27,306 (2,612)	25,916 (2,487)	20,906 (2,002)	26,908 (3,218)	14,070 (1,341)
Completeness[a] (%)	99.3 (98.5)	100.0 (100.0)	100.0 (100.0)	99.8 (99.5)	100.0 (100.0)
I/σI[a]	16.6 (2.2)	14.1 (2.0)	23.5 (2.0)	17.2 (1.8)	19.6 (2.0)
R_{merge}[a]	0.059 (0.877)	0.068 (0.989)	0.045 (1.085)	0.058 (1.255)	0.101 (1.387)
CC (1/2)	0.999 (0.767)	0.999 (0.867)	1.000 (0.833)	1.000 (0.738)	0.999 (0.798)
Redundancy[a]	8.7 (8.5)	11.1 (11.6)	11.8 (12.5	9.6 (9.4)	13.8 (14.2)
Refinement					
No. atoms in refinement (P/L/O)[b]	2,199/ 46/ 185	2,221/ 28/ 128	2,224/ 42/ 44	4,231/ 42/ 36	2,185/ -/ 14
B factor (P/L/O)[b] ($Å^2$)	43/ 45/ 49	52/ 78/ 51	73/ 99/ 59	95/ 114/ 71	97/ -/ 68
R_{fact} (%)	17.6	19.7	22.2	21.6	23.8
R_{free} (%)	20.1	24.5	28.2	26.3	28.2
rms deviation bond[c] (Å)	0.015	0.014	0.011	0.011	0.012
rms deviation angle[c] (°)	1.5	1.3	1.2	1.3	1.1
Crystallization condition	1.4 M ammonium sulfate, 0.1 M tris 8.0	1.6 M ammonium sulfate, 0.1 M tris 7.5	1.6 M ammonium sulfate, 0.1 M tris 8.0	30% PEG 3350, 0.15 M sodium citrate	27% PEG 3350, 0.15 M sodium citrate

[a] Values in brackets show the statistics for the highest resolution shells.
[b] P/L/O indicate protein, ligand of interest and others (water and solvent molecules), respectively.
[c] rms indicates root-mean-square.

HTRF-based PPARγ co-regulator recruitment and dimerization assays

PPARγ co-regulator recruitment screen. A homogeneous time-resolved fluorescence resonance energy transfer (HTRF) assay system was used to study the recruitment of co-regulatory peptides to the PPARγ LBD as described previously[1]. Biotinylated recombinant PPARγ LBD protein (expressed as described previously[11]) was stably coupled to terbium cryptate as streptavidin conjugate (Tb-SA; Cisbio Bioassays, Codolet, France) serving as FRET donor. Assay solutions were prepared in HTRF assay buffer (25 mM HEPES pH 7.5; 150 mM KF, 10% (w/v) glycerol) supplemented with 5 mM DTT and 0.1% (w/v) CHAPS and contained recombinant biotinylated PPARγ (final concentration 3 nM), Tb-SA (3 nM), the respective fluorescein-labeled co-regulator peptide (100 nM), and 1% DMSO with test compounds or DMSO alone as negative control. The co-regulator peptides fused to fluorescein as FRET acceptor were purchased from ThermoFisher Scientific (Life Technologies GmbH, Darmstadt, Germany). All experiments were performed in 384 well format using white flat bottom polystyrene microtiter plates (Greiner Bio-One, Frickenhausen, Germany). Each sample was tested in four technical replicates. After 2 hours incubation at room temperature, fluorescence intensity (FI) was measured at 520 nm for fluorescein acceptor fluorescence and at 620 nm for Tb-SA donor fluorescence on a SPARK plate reader (Tecan Deutschland GmbH) after excitation at 340 nm. FI520nm was divided by FI620nm and then multiplied by 10,000 to obtain a dimensionless HTRF signal. The following co-regulator peptides were used: steroid receptor co-activator (SRC) 1-1, Fluorescein-KY SQTSHKLVQLLTTTAEQQL-OH; SRC 1-2, Fluorescein-LTARHKILHRLLQEGSPSD-OH; SRC 1-3, Fluorescein-ESKD HQLLRYLLDKDEKDL-OH; SRC 1-4, Fluorescein-GPQTPQAQQKSLLQQLLTE-OH; SRC 2-1, Fluorescein-DSKGQTKLLQLLTTKSDQ M-OH; SRC 2-2, Fluorescein-LKEKHKILHRLLQDSSSPV-OH; SRC 2-3, Fluorescein-KKKENALLRYLLDKDDTKD-OH; SRC 3-1, Fluorescein - ESKGHKKLLQLLTCSSDDR-OH; SRC 3-2, Fluorescein-LQEKHRILHKLLQNGNSPA-OH; SRC 3-3, Fluorescein-KKENNALLRYLLDRDDPSD-OH; nuclear receptor co-repressor (NCOR) ID1, Fluorescein-RTHRLITLADHICQIITQDFARN-OH; NCOR ID2, Fluorescein- DPASNLGLEDIIRKALMGSFDDK-OH; silencing mediator for retinoid and thyroid hormone receptor (SMRT) ID1, Fluorescein-GHQRVVTLAQHISEVITQDYTRH-OH; SMRT ID2, Fluorescein - HASTNMGLEAIIRKALMGKYDQW-OH; CREB-binding protein 1 (CBP-1), Fluorescein-AASKHKQLSELLRGGSGSS-OH; C33, Fluorescein-HVEMHPLLMGLLMESQWGA-OH; D11-FXXLF, Fluorescein-VESGSSRFMQLFMANDLLT-OH; D22, Fluorescein- LPYEGSLLLKLLRAPVEEV-OH; EAB1, Fluorescein-SSNHQSSRLIELLSR-OH; EA2, Fluorescein-SSKGVLWRMLAEPVSR-OH; androgen receptor-associated protein 70 (ARA70), Fluorescein-SRETSEKFKLLFQSYNVND-OH; N-terminal sequence of androgen receptor (AR N-term), Fluorescein-SKTYRGAFQNLFQSVREVI-OH; peroxisome proliferator-activated receptor gamma co-activator 1-alpha (PGC1a), Fluorescein-EAEEPSLLKKLLLAPANTQ-OH; nuclear receptor co-activator 6 (NCoA6, also termed PRIPRAP250), Fluorescein-VTLTSPLLVNLLQSDISAG-OH; nuclear receptor interacting protein 1 (NRIP1, also termed RIP140, interaction motif L6), Fluorescein-SHQKVTLLQLLLGHKNEEN-OH; RIP140L8, Fluorescein-SFSKNGLLSRLLRQNQDSY-OH; TB3, Fluorescein-SSVASREWWVRELSR-OH; thyroid hormone receptor associated protein (TRAP) TRAP220/DRIP-1, Fluorescein-KVSQNPILTSLLQITGNGG-OH; TRAP220/DRIP-2, Fluorescein-NTKNHPMLMNLLKDNPAQD-OH. For experiments involving covalent antagonist

GW9662, PPARγ (3 nM) in fully supplemented HTRF buffer was pre-incubated with 10 µM GW9662 for 48 h at 4 °C in presence of 0.125% DMSO.

Dose-dependent PPARγ co-regulator recruitment assays involving sGFP-labeled PPARγ. Dose-dependent modulation of co-regulator recruitment as shown in Figure S7 was investigated in a different HTRF-based setup utilizing PPARγ LBD with N-terminal fusion to superfolder GFP (sGFP-PPARγ; expressed as described previously[11]) with sGFP serving as the FRET acceptor. Peptides derived from CBP-1 coactivator motif 1 [CBP; biotin-NLVPDAASKHKQLSELLRGGSGS-OH], and SMRT interaction domain 2 [SMRT-ID2; biotin-SQAVQEHASTNMGLEAIIRKALMGKYDQW-OH] were purchased from Eurogentec (Seraing, Belgium) and coupled via streptavidin to Terbium cryptate. Assay solutions were prepared in 25 mM HEPES, pH 7.5, 150 mM KF, 5% (w/v) glycerol, 5 mM DTT, and 0.1% (w/v) CHAPS and contained Tb-SA (12 nM), the respective biotin-labeled peptide (12 nM), either 100 nM (for CBP) or 24 nM (for SMRT) sGFP-PPARγ protein, and 1% DMSO with test compounds or DMSO alone as negative control. Each sample was tested in three technical replicates. After 24 h incubation at RT, the fluorescence intensities (FI) at 520 nm and 620 nm were recorded and the HTRF determined as described above.

PPARγ-RXRα heterodimer formation assay. Influence of **2** on the formation of the PPARγ-RXRα heterodimer was investigated by titrating sGFP-RXRα-LBD (up to 300 nM, FRET acceptor) in presence of biotinylated PPARγ LBD[11] (0.375 nM), and Tb-SA (0.75 nM). The total sGFP content was kept constant at 300 nM by adding free sGFP. Assays were performed in HTRF assay buffer with 10% (w/v) glycerol supplemented with 5 mM DTT and 0.1% (w/v) CHAPS with 1% DMSO and test compounds at the indicated concentrations or DMSO alone as reference. Each sample was tested in three technical replicates. After 2 h incubation at RT, the fluorescence intensities (FI) at 520 nm and 620 nm were recorded and the HTRF determined as described above.

Binding assays

Differential Scanning Fluorimetry. Thermal stability of the recombinant PPARγ LBD (prepared as described previously[12]) and stabilization by test compounds was studied by differential scanning fluorimetry on an Mx3005p real-time PCR instrument (Stratagene, San Diego, CA, USA) according to a published protocol[13]. Recombinant PPARγ LBD protein (final concentration 2 µM) in buffer (10 mM HEPES pH 7.5; 100 mM NaCl) was mixed with SYPRO Orange dye (1:1000 dilution), DMSO (final concentration 5%) and test compounds (**2**, pioglitazone and mixtures at varying concentrations). Temperature was increased over 71 cycles (1 °C/cycle). All samples were tested in three independent experiments and control experiments without PPARγ-LBD were conducted to observe potential non-specific interactions between test compounds and the dye. The amplification plots were analyzed using a Boltzmann fit to obtain the melting points (T_m) and to calculate ΔT_m corresponding to T_m (compound) - T_m (untreated).

Isothermal titration calorimetry. ITC experiments were conducted on an Affinity ITC instrument (TA Instruments, New Castle, DE) at 25 °C with a stirring rate of 75 rpm. PPARγ LBD protein (20 µM, prepared as described previously[1]) in buffer (20 mM Tris pH 7.5, 150 mM NaCl, 5% glycerol) containing 5% DMSO was titrated with the test compounds (100 µM in the same buffer containing 5% DMSO) in 26 injections (1 × 1

µL and 25 × 5 µL) with an injection interval of 150 s. To determine binding to the GW9662-bound PPARγ LBD, the protein (100 µM) was incubated at 4 °C for 24 h prior to the ITC experiment in the above described buffer supplemented with 250 µM GW9662. ITC was then conducted as described above using buffer supplemented with 50 µM GW9662. Binding of GW9662 was verified by titration of the GW9662-bound PPARγ LBD with pioglitazone under the same conditions which showed no heat of binding. As control experiments, the test compounds were titrated into the respective buffer, and the respective buffer was titrated to the PPARγ LBD proteins under otherwise identical conditions. The ITC results were analyzed using NanoAnalyze software (TA Instruments, New Castle, DE) with a sequential two-site binding model (**1**-PPARγ) or an independent binding model (**1**-PPARγ/GW9662, **2**-PPARγ, **2**-PPARγ/GW9662).

MS-based PPARγ ligand binding assay. PPARγ LBD (at concentrations of 0.2 µM or 1 µM) was incubated with ligands in Tris buffer (20 mM Tris, 200 mM NaCl, 0.5 mM TCEP, 5% (v/v) glycerol, 1% (v/v) DMSO, pH 7.5) in a total volume of 110 µL for 1 h at 25 °C in a shaking water bath. In parallel, incubation was performed with previously denatured protein (80 °C, 30 min, water bath) under otherwise identical conditions. After transfer of 100 µL of the binding samples to Microcon 10 kDa 0.5 mL centrifugal filters containing an Ultracel regenerated cellulose membrane (Merck, Darmstadt, Germany) ultrafiltration was performed at 14000 g for 40 min leading to a remaining volume of about 5 µL. Next, each filter was put into another polypropylene tube and 10 µL ammonium acetate buffer (154 mM, pH 7.4) was added on top of each filter before intense vortexing for 10 s. To separate the remaining residue on top of the membrane, the filter units were flipped over, so that the flow direction was opposite to the ultrafiltration step and centrifuged at 4000 g for 1 min. To the thus obtained samples, 80 µL mobile phase (see below) were added. After centrifugation at 25142 g for 10 min, aliquots of each supernatant were supplemented with JP147 (compound 28 from ref[4], final concentration 10 nM) as internal standard and diluted with mobile phase (see below). Quantification by LC-ESI-MS/MS was achieved using an API 3200 QTrap triple quadrupole mass spectrometer (Sciex, Darmstadt, Germany) coupled to an Agilent 1100 HPLC system (Agilent, Waldbronn, Germany) and a SIL-20A/HT autosampler (Shimadzu, Duisburg, Germany) controlled by the Analyst software (v.1.6.3) at an injection volume of 10 µL. A Triart C18 column (3 µm, 50 mm x 2 mm, YMC Europe, protected with a 0.5 µm and a 0.2 µm frit) was used as stationary phase and 0.1% HCOOH and H_3CCN (40/60, v/v) as mobile phase at a flow rate of 400 µL/min. MS detection was performed under positive ESI conditions in the MRM mode recording *m/z* 416.1 → 105.1 (**2**), *m/z* 357.2 → 134.1 (pioglitazone) and *m/z* 382.2 → 310.1 (JP147).

Reporter gene assays

Hybrid reporter gene assays. Gal4-hybrid reporter gene assays were performed as described previously using the plasmids pFA-CMV-hTHRα-LBD[12], pFA-CMV-hTHRβ-LBD[12], pFA-CMV-hRARα-LBD[14], pFA-CMV-hRARβ-LBD[14], pFA-CMV-hRARγ-LBD[14], pFA-CMV-hPPARα-LBD[15], pFA-CMV-hPPARγ-LBD[15], pFA-CMV-hPPARδ-LBD[15], pFA-CMV-revERBα-LBD, pFA-CMV-hRORα-LBD[16], pFA-CMV-hRORβ-LBD[16], pFA-CMV-hRORγ-LBD[16], pFA-CMV-hLXRα-LBD[17], pFA-CMV-hLXRβ-LBD[17], pFA-CMV-hFXR-LBD[18], pFA-CMV-hVDR-LBD[14], pFA-CMV-hCAR-LBD[14], pFA-CMV-hHNF4α-

LBD[19], pFA-CMV-hRXRα-LBD[20], pFA-CMV-hRXRβ-LBD[20], pFA-CMV-hRXRγ-LBD[20], pFA-CMV-hTR2-LBD[21], pFA-CMV-hTR4-LBD[21], pFA-CMV-hTLX-LBD[21], pFA-CMV-hNur77-LBD[22], pFA-CMV-hNurr1-LBD[22], pFA-CMV-hNOR1-LBD[22], and pFA-CMV-hLRH1-LBD encoding the hinge region and the ligand binding domain (LBD) of the canonical isoform of nuclear receptors. pFR-Luc (Stratagene) was used as reporter plasmid and pRL-SV40 (Promega) for normalization of transfection efficiency and cell growth. HEK293T cells (German Collection of Microorganisms and Cell Culture GmbH, DSMZ) were cultured in Dulbecco's modified Eagle's medium (DMEM), high glucose supplemented with 10% fetal calf serum (FCS), sodium pyruvate (1 mM), penicillin (100 U/mL), and streptomycin (100 µg/mL) at 37 °C and 5% CO_2 and seeded in 96-well plates (3×10^4 cells/well). Medium was changed to Opti-MEM without supplements and cells were transiently transfected with one pFA-CMV-hNR-LBD clone, pFR-Luc and pRL-SV40 using Lipofectamine LTX reagent (Invitrogen) according to the manufacturer's instructions. Five hours after transfection, cells were incubated with the test compounds in Opti-MEM supplemented with penicillin (100 U/mL), streptomycin (100 µg/mL) and 0.1% DMSO. Each sample was set up in duplicates and tested in at least three independent experiments. After 16 h incubation, luciferase activity was measured using the Dual-Glo Luciferase Assay System (Promega) according to the manufacturer's protocol on a Tecan Spark luminometer (Tecan Deutschland GmbH, Germany). Firefly luminescence was divided by Renilla luminescence and multiplied by 1000 resulting in relative light units (RLU) to normalize for transfection efficiency and cell growth. Fold activation was obtained by dividing the mean RLU of test compound by the mean RLU of the untreated control and relative activation was calculated by dividing the fold activation of a test sample by the fold activation of the respective reference agonist. The following reference ligands were used: THRα/THRβ – 1 µM T3; RARα/RARβ/RARγ – 1 µM tretinoin; PPARα – 1 µM GW7647; PPARγ – 1 µM pioglitazone; PPARδ – 1 µM L165,041; RORγ – 1 µM SR1001; RORα/RORβ/LXRα/LXRβ – 1 µM T0901317; FXR – 1 µM GW4064; VDR – 1 µM calcitriol; CAR – 1 µM CITCO; HNF4α – 1 µM compound 9[19]; RXRα/RXRβ/RXRγ – 1 µM bexarotene; TLX – 100 µM propranolol; Nur77/Nurr1/NOR1 – 100 µM amodiaquine. For dose-response curve fitting and calculation of EC_{50} values, the equation "[Agonist] versus response (variable slope - four parameters)" was performed in GraphPad Prism (version 7.00, GraphPad Software, La Jolla, CA, USA).

PPRE assay. Activation of the PPAR response element (PPRE) was studied as described previously[4] using the reporter plasmid PPRE1-pGL3 encoding firefly luciferase under control of the human PPRE. pRL-SV40 was used for normalization of transfection efficiency and cell growth. HepG2 cells (DSMZ) were grown in DMEM high glucose supplemented with 10% FCS, sodium pyruvate (1 mM), penicillin (100 U/mL) and streptomycin (100 µg/mL) at 37 °C and 5% CO_2. 24 h before transfection, cells were seeded in 96-well plates (1.25×10^4 cells/well) pre-coated with Collagen G solution. Before transfection, the medium was replaced with Opti-MEM without additives. Transient transfection was performed using Lipofectamine 3000 reagent (Invitrogen) according to the manufacturer's protocol with PPRE1-pGL3 and pRL-SV40 (Promega). 5 h after transfection, cells were incubated with Opti-MEM supplemented with penicillin (100 U/mL) and streptomycin (100 µg/mL) containing 0.1% DMSO and the respective test compound or 0.1% DMSO alone as an untreated control for 16 h. Each sample was tested in duplicate, and each experiment was repeated independently three times. Luciferase activity measurement and data analysis were performed as described for the hybrid reporter gene assays.

PPARγ phosphorylation at Ser273

HEK293T cells were seeded in 6-well plates (3 x 10^5 cells/well) in DMEM high glucose, supplemented with sodium pyruvate (1 mM), penicillin (100 U/mL), streptomycin (100 µg/mL) and 10% FCS at 37 °C and 5% CO_2. After 24 h, cells were treated with rosiglitazone (1 µM) or **2** (20 µM) in Opti-MEM supplemented with penicillin (100 U/mL), streptomycin (100 µg/mL) and 0.1% DMSO or with the supplemented medium alone. Each sample was prepared in three biologically independent repeats. After 16 h, cells were harvested, centrifuged at 1000 g for 10 min and frozen at -80 °C as dry pellets until further processing. For protein extraction, pellets were resuspended in 100 µL complete radioimmunoprecipitation assay buffer (10 mL Pierce RIPA buffer supplemented with 1 tablet Pierce Protease and Phosphatase Inhibitor, ThermoFisher #A32959), thoroughly vortexed, and incubated at 4 °C and 600 rpm horizontal shaking for 15 min. After subsequent centrifugation at 14,000 g and 4 °C for 10 min, supernatants were harvested, mixed with 25 µL 5X Pierce TM Lane Marker Reducing Sample Buffer (ThermoFisher #39000), and heated to 95 °C for 5 min. Samples were stored at -80 °C until further processing. Sodium dodecyl sulfate (SDS) polyacrylamide gel electrophoresis was conducted using a 12% polyacrylamide gel loaded with 15 µL protein extract at 100 V for 20 min and 200 V for 40 min in running buffer (25 mM TRIS, 192 mM glycin, 0.1% w/v SDS, pH 8.3). Right before tank blotting of the separated protein to a methanol-activated polyvinylidene fluoride (PVDF) membrane (Immobilon®-FL PVDF-Membran, Merck, #05317), gel and membrane were equilibrated in transfer buffer (125 mM TRIS, 970 mM glycin) for 2 min. Tank blotting using transfer buffer drenched Whattmann-paper was conducted at 80 V and 4 °C over night. The PVDF membrane was washed 4 times for 10 min in Tris-buffered saline with 0.5% Tween 20 (TBST) and incubated in TBST with 5% BSA and either anti-PPARγ (Ser273) antibody (Bioss Antibodies #bs-4888R, diluted 1:1000), or anti-GAPDH (Cell Signaling Technology, clone D16H11, diluted 1:1000) over night at 4 °C, respectively. After repeating the washing step as described above, the membrane was incubated with horseradish peroxidase-conjugated secondary antibody (Sigma Aldrich #12-348, diluted 1:4000 in TBST and 5% skimmed milk) for 1 h at room temperature. After washing in TBST, the membrane was submerged in enhanced chemiluminescence solution (100 mM Tris/HCl pH 8.8, 2.5 mM luminol, 0.4 mM p-cumaric acid, 2.6 mM hydrogenperoxide) for 1 min and signal was detected using a ChemiDoc Imaging System (BioRad).

Toxicity assay

COS-7 (DSMZ #ACC 60) cells were grown in DMEM high glucose, supplemented with 10% FCS, sodium pyruvate (1 mM), penicillin (100 U/mL), and streptomycin (100 µg/mL) at 37 °C and 5% CO_2. The day before the experiment, cells were seeded in 96-well plates (5 × 10^4 cells per well) in culture medium with reduced serum content (0.2%). The next day, medium was changed, maintaining the low serum content, and additionally containing 0.1% DMSO and the respective test compound or 0.1% DMSO alone as untreated control. After incubation for 24 h, the medium was aspirated, the wells were washed once with 100 µL PBS, and incubated for 30 min with PBS containing either 1 µM NucView® 405 fluorogenic caspase-3 substrate (#10405, Biotium, Fremont, USA) or 0.5 µg/mL propidium iodide (#P4864, Merck, Darmstadt, Germany) to detect apoptosis and non-regulated forms of cell death, respectively. After incubation, a total of 6 fluorescence images per well at 10X magnification were taken

to detect NucView® (Ex: 381–400 nm, Em: 414–450 nm) and propidium iodide (Ex: 543–566 nm, Em: 580–611 nm), respectively, using on a Tecan Spark Cyto (Tecan Group AG). Reference readings for background correction and detection of auto-fluorescence were taken at the given wavelength prior to staining. Additionally, cell confluence was determined before test compound administration, after the first medium exchange, 24 h after test compound administration, and after fluorescence imaging using a Tecan Spark Cyto, to observe cell loss due to test compound administration and cell handling.

Adipocyte-derived mesenchymal stem cell differentiation

Cell culture and treatment: Differentiation experiments of ASC52telo, hTERT cells (ATCC® SCRC-4000™) were conducted according to a previously described procedure[23]. In brief, cells were grown in DMEM high glucose, supplemented with 10% fetal calf serum, sodium pyruvate (1 mM), penicillin (100 U/mL), and streptomycin (100 µg/mL) at 37 °C and 5% CO_2. Cells were seeded in standard culture medium at a density of 5,000 cells per well in 96-well plates. After adherence overnight, cells were incubated with differentiation medium, composed of standard culture medium supplemented with human insulin (10 µg/mL, #I3536, Merck KgaA, Darmstadt, Germany), dexamethasone (1 µM, #D4902, Merck KgaA, Darmstadt, Germany,), isobutylmethylxanthine (0.5 mM, #I5879, Merck KgaA, Darmstadt, Germany), DMSO (final concentration 0.1%) and the respective test compounds. The differentiation medium was exchanged every 48-72 h for a total of six cycles in 13 days. The test compounds were supplemented freshly with every medium exchange. From day 14 until day 22 of culture, cells were kept in maintenance medium, composed of standard culture medium supplemented with human insulin (10 µg/mL) without additional treatment. The maintenance medium was exchanged every 48-72 h for a total of four cycles in nine days.

Oil Red O staining: After the 21-day differentiation procedure and test compound treatment, cells were washed with phosphate buffered saline (PBS) once and fixed with formalin (10%, stabilized with methanol, 100 µL per well, #15071, Morphisto GmbH, Offenbach am Main, Germany) for 15 min at room temperature. The fixing solution was aspirated, and the fixed cells were washed twice with 40% 2-propanol with the second wash step incubating for 30 min at room temperature to equilibrate the specimens for staining. Oil Red O (#O0625, Merck KgaA, Darmstadt, Germany) was prepared at 10 mg/mL in 2-propanol, filtered with grade 595 Whatman® filter paper (#311611, Schleicher & Schuell GmbH, London, UK) and a 0.2 µm syringe filter (FP 30/0,2 CA-S, #10462200, Schleicher & Schuell GmbH, London, UK), and diluted with ddH_2O to a final concentration of 0.4% Oil Red O and 40% 2-propanol. Upon equilibration, specimens were incubated with 50 µL of 0.4% Oil Red O solution for 1 h at room temperature before the staining solution was aspirated and the wells were washed with ddH_2O 2-3 times to remove precipitated Oil Red O crystals. Specimens were kept in ddH_2O for subsequent analysis. For each well, multiple pictures were taken at a 4X magnification using a Motic®AE31E inverted microscope and a Moticam 1080 (Motic Hong Kong Ldt.). Images were dichromized and the red channel was extracted for analysis using ImageJ 1.53q. Percent Oil Red O-positive stained area was evaluated by generating binary pictures via application of a suitable threshold on the extracted pictures. The mean value of three technical replicates was calculated for

a single biological replicate. Each sample was tested in three biologically independent experiments (n=3).

Differential gene expression analysis of hepatocytes

Sample preparation. HepG2 cells (DSMZ) were cultured in DMEM, high glucose supplemented with 10% fetal calf serum (FCS), sodium pyruvate (1 mM), penicillin (100 U/mL), and streptomycin (100 µg/mL) at 37 °C and 5% CO_2 and seeded in 6-well plates (1.0×10^6 cells/well). At 24 h after seeding, the medium was replaced with minimal essential medium (MEM) containing 1% charcoal-stripped FCS, penicillin (100 U/mL), and streptomycin (100 µg/mL). After 48 h, the medium was again exchanged for MEM with the same additives as before, additionally containing 0.1% DMSO and compound **2** (20 µM) or 0.1% DMSO alone as a control. Each treatment was performed in four biologically independent samples (n = 4). After an incubation period of 12 h, cells were harvested, washed twice with cold phosphate buffered saline (PBS), and used for RNA extraction with the E.Z.N.A.® Total RNA Kit I (R6834-02, Omega-Bio-Tek Inc., Norcross, GA, USA).

Unbiased RNA sequencing and downstream analysis. RNAseq was performed by Novogene (Cambridge, UK) on a fee-for-service basis. A total amount of 1 µg RNA per sample was used as input material for the RNA sample preparations. Sequencing libraries were generated using NEBNext® Ultra TM RNA Library Prep Kit for Illumina® (NEB, USA) following manufacturer's recommendations and index codes were added to attribute sequences to each sample. Briefly, mRNA was purified from total RNA using poly-T oligo-attached magnetic beads. Fragmentation was carried out using divalent cations under elevated temperature in NEBNext First Strand Synthesis Reaction Buffer (5X). First strand cDNA was synthesized using random hexamer primer and M-MuLV Reverse Transcriptase (RNase H). Second strand cDNA synthesis was subsequently performed using DNA Polymerase I and RNase H. Remaining overhangs were converted into blunt ends via exonuclease/polymerase activities. After adenylation of 3' ends of DNA fragments, NEBNext Adaptor with hairpin loop structure were ligated to prepare for hybridization. In order to select cDNA fragments of preferentially 150~200 bp in length, the library fragments were purified with AMPure XP system (Beckman Coulter, Beverly, USA). Then 3 µL USER Enzyme (NEB, USA) was used with size-selected, adaptor-ligated cDNA at 37 °C for 15 min followed by 5 min at 95 °C before PCR. Then PCR was performed with Phusion High-Fidelity DNA polymerase, Universal PCR primers and Index (X) Primer. At last, PCR products were purified (AMPure XP system) and library quality was assessed on the Agilent Bioanalyzer 2100 system. The clustering of the index-coded samples was performed on a cBot Cluster Generation System using PE Cluster Kit cBot-HS (Illumina) according to the manufacturer's instructions. After cluster generation, the library preparations were sequenced on an Illumina platform and paired-end reads were generated. Raw data (raw reads) of FASTQ format were firstly processed through fastp. In this step, clean data (clean reads) were obtained by removing reads containing adapter and poly-N sequences and reads with low quality from raw data. At the same time, Q20, Q30 and GC content of the clean data were calculated. All the downstream analyses were based on the clean data with high quality. Reference genome and gene model annotation files were downloaded from genome website browser (NCBI/UCSC/Ensembl) directly. Paired-end clean reads were aligned to the reference genome using the Spliced Transcripts Alignment to a Reference (STAR)

software, which is based on a previously undescribed RNA-seq alignment algorithm that uses sequential maximum mappable seed search in uncompressed suffix arrays followed by seed clustering and stitching procedure. FeatureCounts was used to count the read numbers mapped of each gene. Then, Reads Per Kilobase of exon model per Million mapped reads (RPKM) of each gene was calculated based on the length of the gene and reads count mapped to this gene. RPKM considers the effect of sequencing depth and gene length for the reads count at the same time and is used for estimating gene expression levels[24]. Differential expression analysis between the two conditions/groups (four biological replicates per condition) was performed using DESeq2 R package which provides statistical routines for determining differential expression in digital gene expression data using a model based on the negative binomial distribution. Genes with an p-value < 0.05 found by DESeq2 were assigned as differentially expressed. Gene Ontology (GO, http://www.geneontology.org/), which is a major bioinformatics classification system to unify the presentation of gene properties and enrichment analysis of differentially expressed genes was implemented by the clusterProfiler, AnnotationDbi, and org.Hs.eg.db R package. GO terms with p-value < 0.05 were considered significantly enriched by differentially expressed genes. The pathview R package on the KEGG pathway project database (http://www.genome.jp/kegg/) was used to visualize pathways regulated (log2 fold change) by different treatments, irrespective of the p-value associated with each gene. The PPARgene database[2] was used to analyze genes regulated by **2**, pioglitazone or GA for the presence of experimentally confirmed or predicted PPAR response elements (results in Table S2).

Observation of FoxO phosphorylation and activity

Cell culture. HepG2 cells (DSMZ) were cultured in DMEM, high glucose supplemented with 10% fetal calf serum (FCS), sodium pyruvate (1 mM), penicillin (100 U/mL), and streptomycin (100 µg/mL) at 37 °C and 5% CO_2. One passage prior to and during experiments, cells were kept on plates coated with collagen G. For coating, culture plates were incubated at 37 °C with a 10 µg/mL solution of collagen G in PBS for 30 min right before cell seeding.

FoxO response element reporter assay. HepG2 cells were seeded in collagen G coated 96-well plates (3 x 10^4 cells/well) in DMEM high glucose, supplemented with sodium pyruvate (1 mM), penicillin (100 U/mL) and streptomycin (100 µg/mL). After 24 h, medium was changed to MEM supplemented with penicillin (100 U/mL) and streptomycin (100 µg/mL). After further 24 h, medium was changed to Opti-MEM without supplements and cells were transiently transfected with FHRE-Luc (Addgene plasmid #1789, 12 ng/well) and pRL-SV40 (Promega, 1 ng/well) using Lipofectamine 3000 (Invitrogen). Four hours after transfection, cells were incubated with the test compounds in MEM supplemented with penicillin (100 U/mL), streptomycin (100 µg/mL) and 0.1% DMSO or the supplemented medium alone. At various time-points after incubation, luciferase activity was measured using the Dual-Glo Luciferase Assay System (Promega) according to the manufacturer's protocol on a Tecan Spark luminometer (Tecan Deutschland GmbH, Germany). Each sample was set up in duplicates and tested in at least three independent experiments. Firefly luminescence was divided by Renilla luminescence and multiplied by 1000 resulting in relative light units (RLU) to normalize for transfection efficiency and cell growth. Relative FHRE

activity was obtained by dividing the mean RLU of treatment samples by the mean RLU of the 0.1% DMSO control.

Protein extraction, SDS-PAGE, and Western blot. HEK293T cells were seeded in 6-well plates (3 x 10^5 cells/well) in DMEM high glucose, supplemented with sodium pyruvate (1 mM), penicillin (100 U/mL), streptomycin (100 µg/mL) and 10% FCS at 37 °C and 5% CO_2. After 24 h, cells were treated with **2** (20 µM) in Opti-MEM supplemented with penicillin (100 U/mL), streptomycin (100 µg/mL) and 0.1% DMSO or with the supplemented medium alone. Each sample was prepared in three biologically independent repeats. After 16 h, cells were harvested, centrifuged at 1000 g for 10 min and frozen at -80 °C as dry pellets until further processing. For protein extraction, pellets were resuspended in 100 µL complete radioimmunoprecipitation assay buffer (10 mL Pierce RIPA buffer supplemented with 1 tablet Pierce Protease and Phosphatase Inhibitor, ThermoFisher #A32959), thoroughly vortexed, and incubated at 4 °C and 600 rpm horizontal shaking for 15 min. After subsequent centrifugation at 14,000 g and 4 °C for 10 min, supernatants were harvested, mixed with 25 µL 5X Pierce TM Lane Marker Reducing Sample Buffer (ThermoFisher #39000), and heated to 95 °C for 5 min. Samples were stored at -80 °C until further processing. Sodium dodecyl sulfate (SDS) polyacrylamide gel electrophoresis was conducted using a 12% polyacrylamide gel loaded with 15 µL protein extract at 100 V for 20 min and 200 V for 40 min in running buffer (25 mM TRIS, 192 mM glycin, 0.1% w/v SDS, pH 8.3). Right before tank blotting of the separated protein to a methanol-activated polyvinylidene fluoride (PVDF) membrane (Immobilon®-FL PVDF-Membran, Merck, #05317), gel and membrane were equilibrated in transfer buffer (125 mM TRIS, 970 mM glycin) for 2 min. Tank blotting using transfer buffer drenched Whattmann-paper was conducted at 80 V and 4 °C over night. The PVDF membrane was washed 4 times for 10 min in Tris-buffered saline with 0.5% Tween 20 (TBST) and incubated in TBST with 5% BSA and either anti-phospho-FoxO3a (Ser253) antibody (Cell Signaling Technology #9466, diluted 1:1000), or anti-GAPDH (Cell Signaling Technology, clone D16H11, diluted 1:1000) over night at 4 °C, respectively. After repeating the washing step as described above, the membrane was incubated with horseradish peroxidase-conjugated secondary antibody (Sigma Aldrich #12-348, diluted 1:4000 in TBST and 5% skimmed milk) for 1 h at room temperature. After washing in TBST, the membrane was submerged in enhanced chemiluminescence solution (100 mM Tris/HCl pH 8.8, 2.5 mM luminol, 0.4 mM p-cumaric acid, 2.6 mM hydrogenperoxide) for 1 min and signal was detected using a ChemiDoc Imaging System (BioRad).

Molecular docking

Molecular docking was performed in Molecular Operating Environment (MOE, version 2020.09, Chemical Computing Group Inc. Montreal, QC, Canada). The X-ray structure of the PPARγ-**1** complex (pdb ID: 8aty) served as template for structure- and docking-based design of **2**. The structure was prepared using the MOE QuickPrep tool with default settings, adjusting the protonation state of the complex. **2** was prepared using the MOE Wash tool with dominant protonation state at pH 7.0; coordinates were rebuilt 3D; existing chirality was maintained. The following settings were used for all docking calculations: Force Field = Amber10:EHT, Receptor = Receptor and Solvent Atoms, Site = Ligand Atoms of **1**, Placement = Template with 100 poses, Refinement = Rigid Receptor, scoring function = GBVI/WSA dG with 10 poses. Redocking of the

crystallized ligand **1** in the orthosteric site (RMSD = 0.39, mean RMSD = 1.57, Score = -8.24) and the alternative site (RMSD = 0.18, mean RMSD = 1.92, Score = -8.67) of PPARγ confirmed suitability of the method. Potential simultaneous binding of 2 and pioglitazone was evaluated by docking pioglitazone to the PPARγ-**2** complex (pdb ID: 8atz). Preparations and docking were performed as described above. However, As no ligand is bound to the orthosteric site of the PPARγ-**2** complex, the thiazolidinedione interactions of pioglitazone with His323, His449 and Ser289 were used as template and the alternative site ligand was used to define excluded volumes. Comparison with the PPARγ-pioglitazone complex 5y2o revealed an RMSD of 3.57 for the experimentally determined binding mode of pioglitazone and the predicted pose in the PPARγ-**2** complex.

NMR and HPLC data of **1**

^{1}H NMR

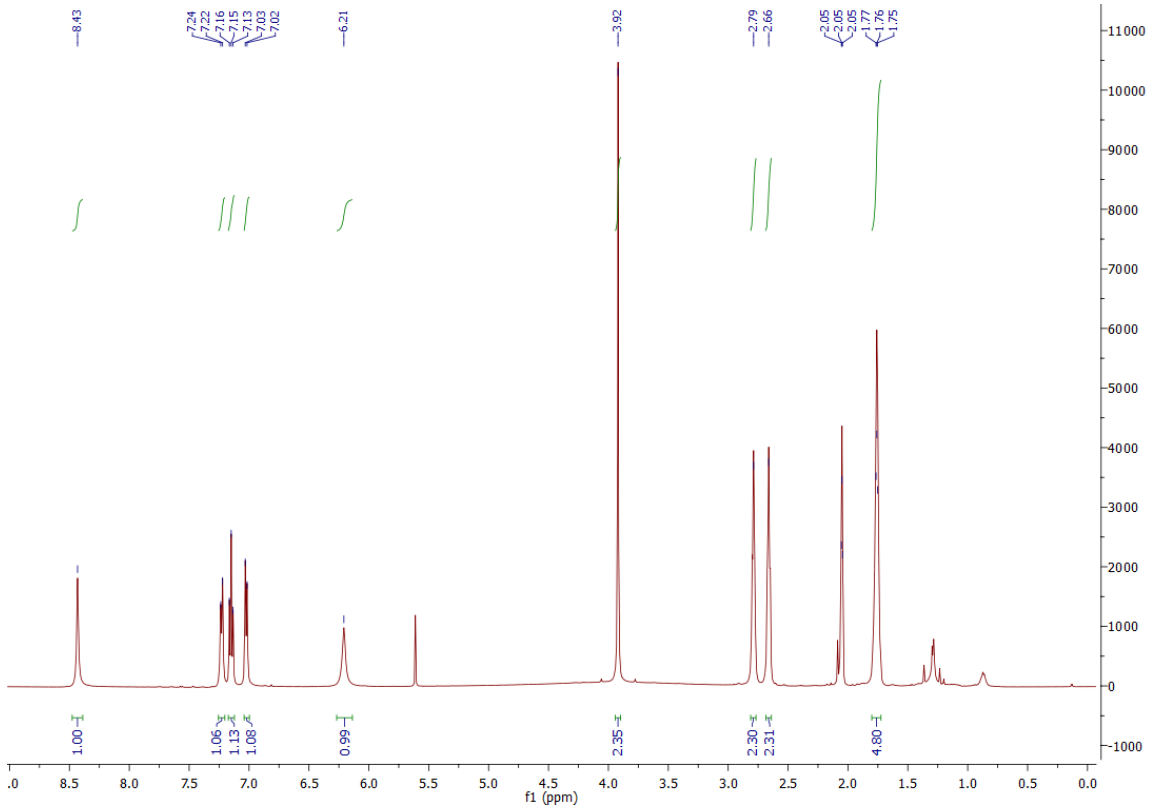

^{13}C NMR

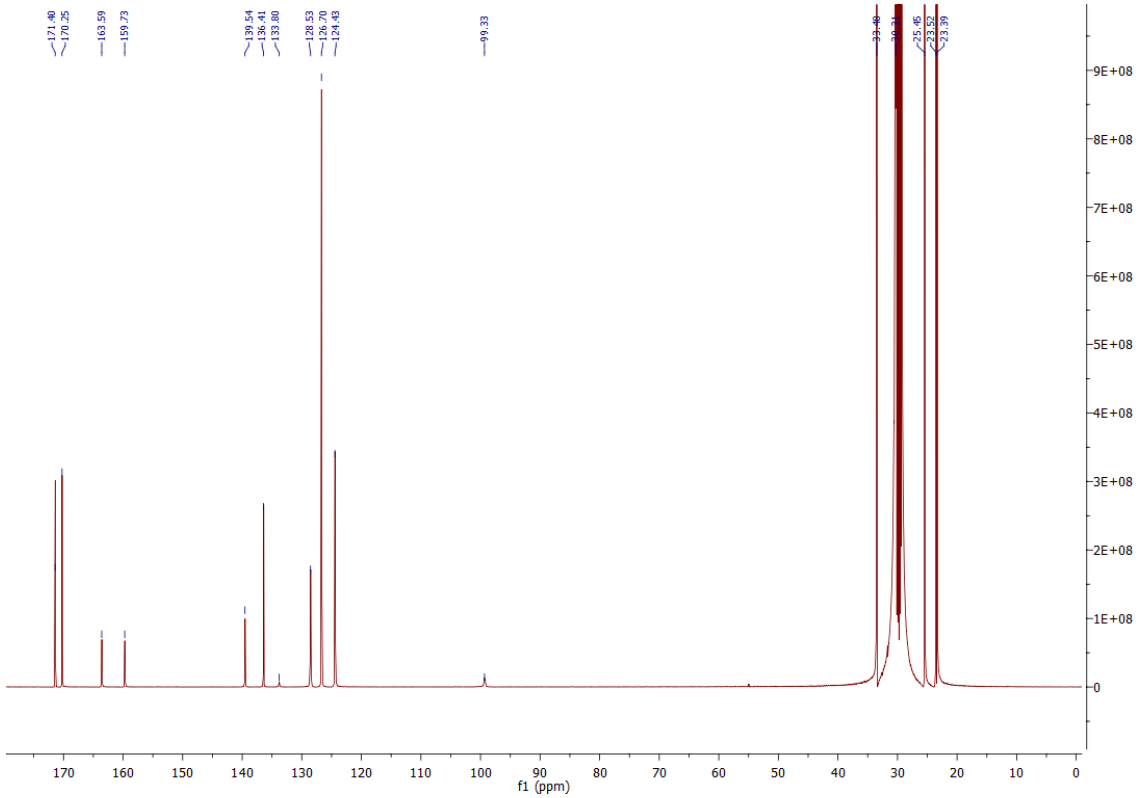

HPLC

Chrom Type: Fixed WL Chromatogram, 254 nm

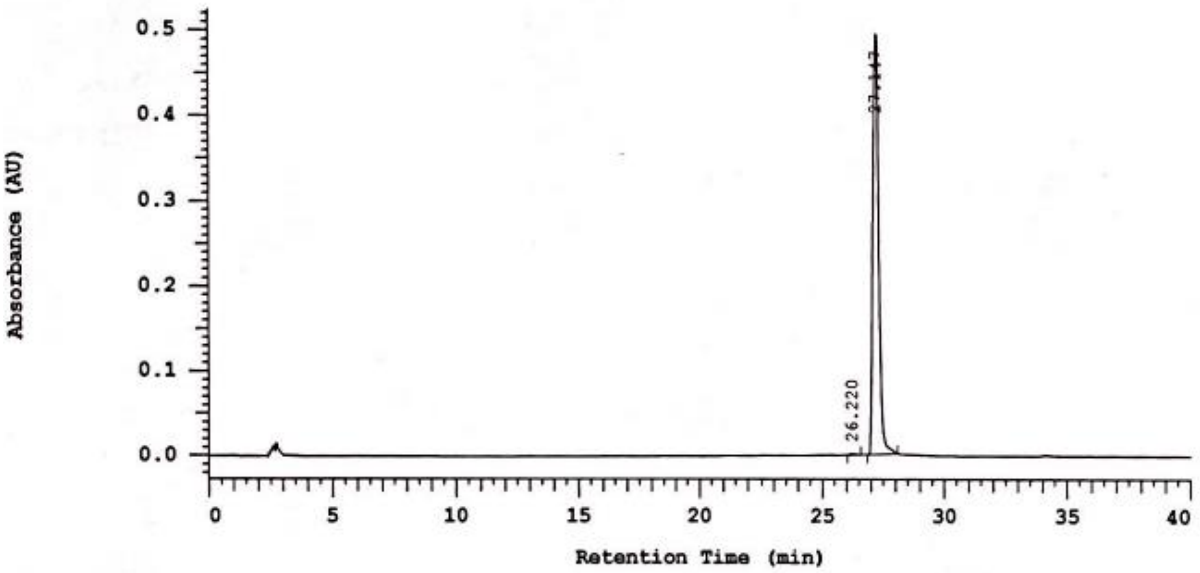

No.	RT	Area	Area %	Height
1	26.220	12067	0.295	793
2	27.147	4073318	99.705	248285
		4085385	100.000	249078

Chrom Type: Fixed WL Chromatogram, 280 nm

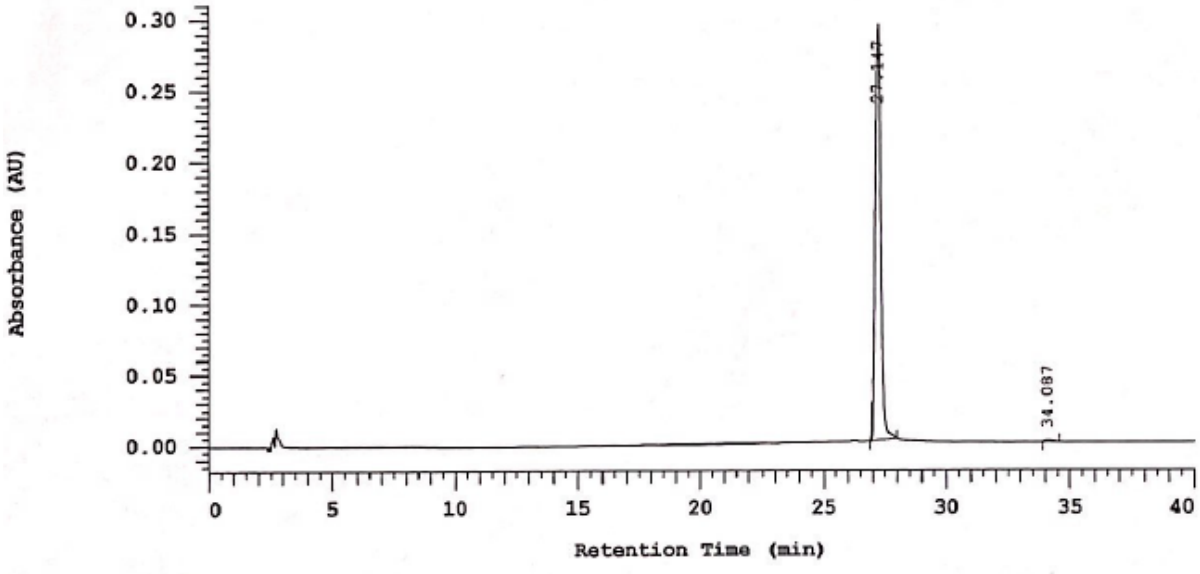

No.	RT	Area	Area %	Height
1	27.147	2382575	99.426	146340
2	34.087	13753	0.574	606
		2396328	100.000	146946

NMR and HPLC data of **2**

^{1}H NMR

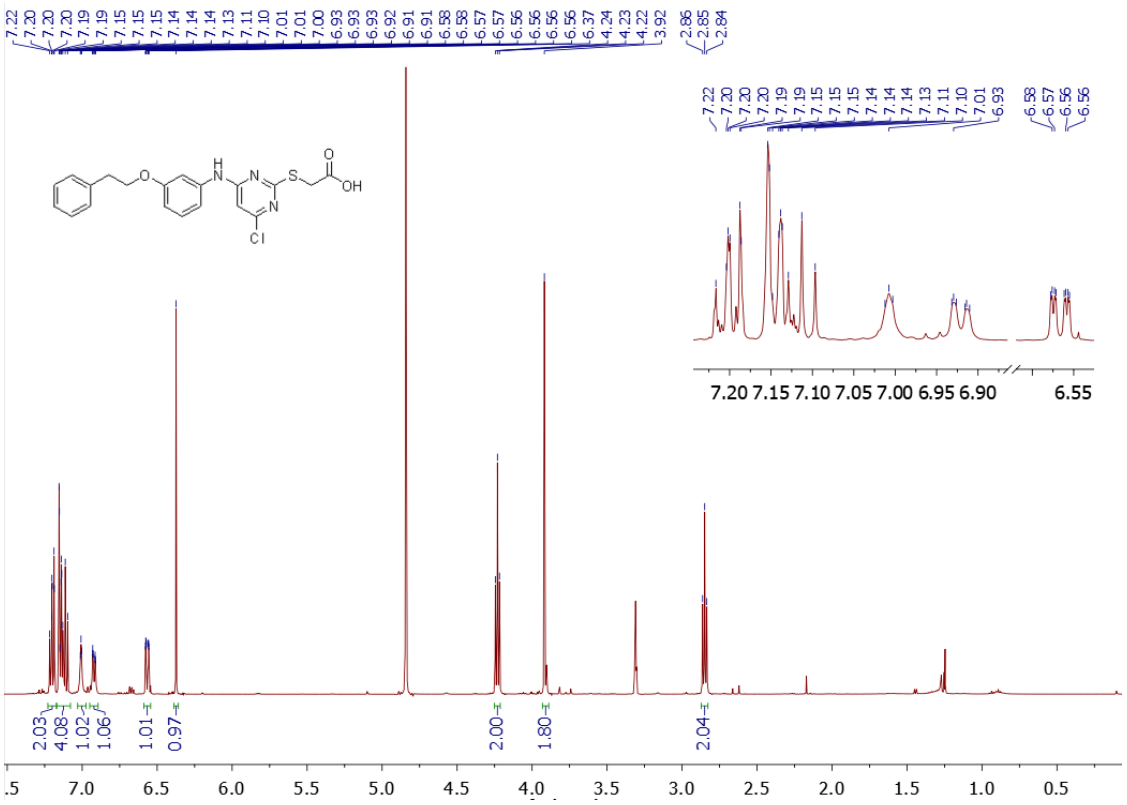

^{13}C NMR

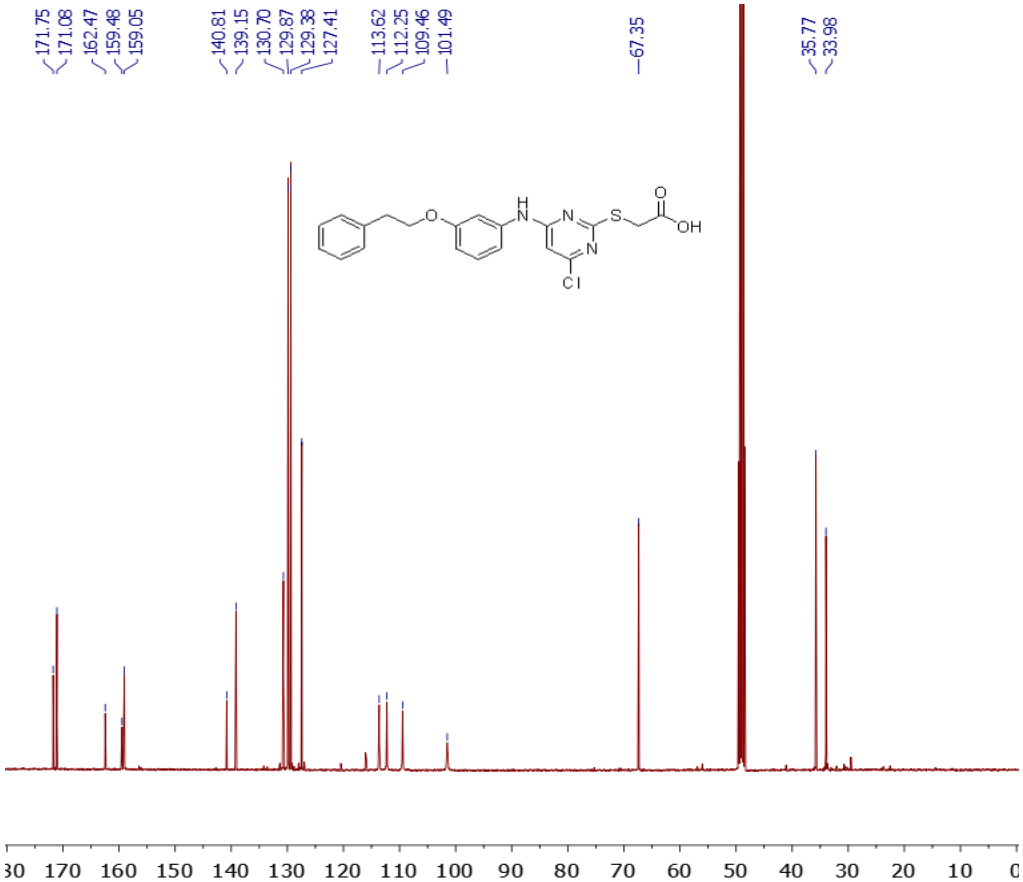

HPLC

Chrom Type: Fixed WL Chromatogram, 254 nm

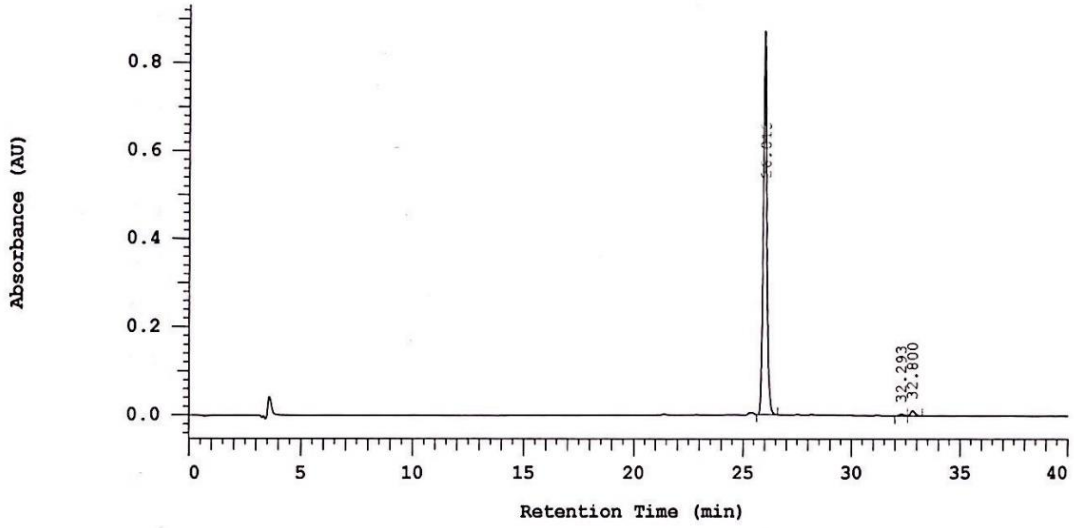

Pump 1: 5160
Pump 1 Solvent A: MeOH
Pump 1 Solvent B: Wasser
Pump 1 Solvent C: MeOH
Pump 1 Solvent D: MeOH

No.	RT	Area	Area %	Height
1	26.013	4875848	97.697	258304
2	32.293	30556	0.612	2272
3	32.800	84378	1.691	6117
		4990782	100.000	266693

Chrom Type: Fixed WL Chromatogram, 280 nm

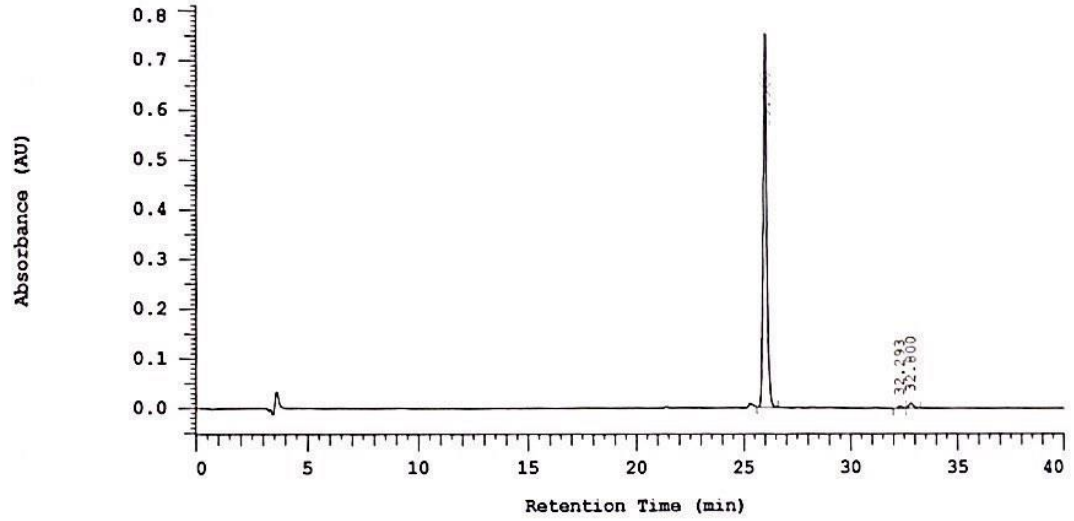

Pump 1: 5160
Pump 1 Solvent A: MeOH
Pump 1 Solvent B: Wasser
Pump 1 Solvent C: MeOH
Pump 1 Solvent D: MeOH

No.	RT	Area	Area %	Height
1	25.960	4238963	97.648	360334
2	32.293	27021	0.622	1985
3	32.800	75073	1.729	5418
		4341057	100.000	367737

Western Blots
(representative)

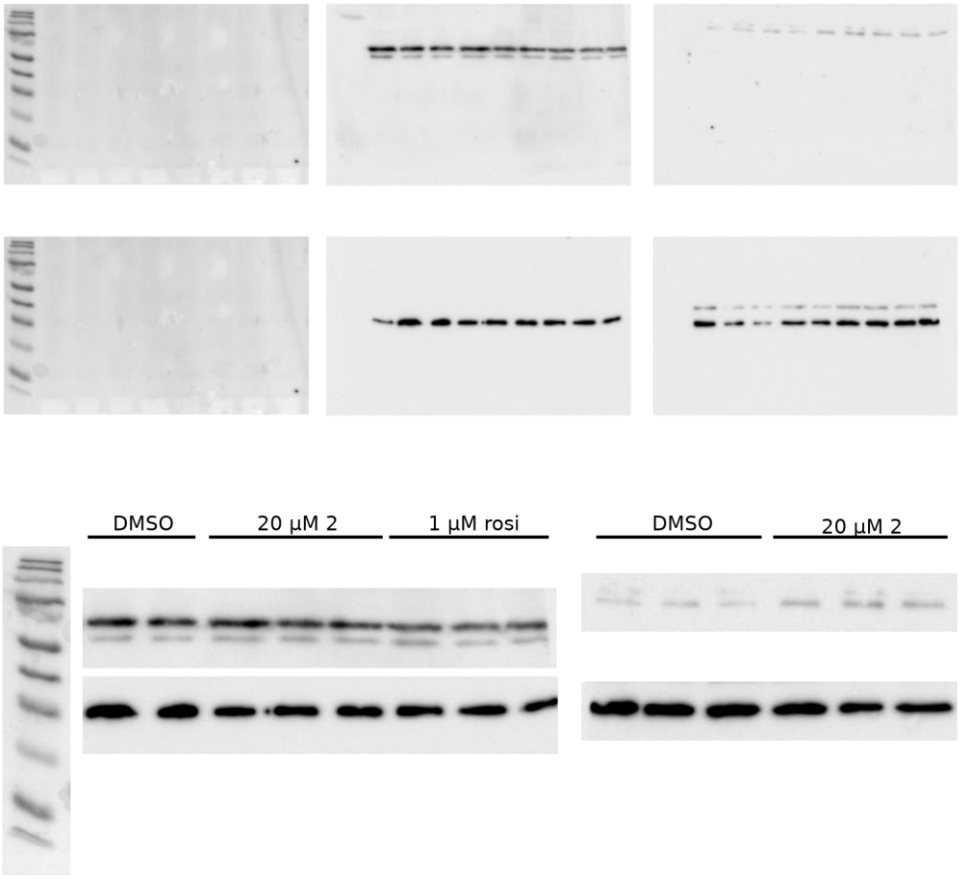

Supplementary References

(1) Willems, S.; Gellrich, L.; Chaikuad, A.; Kluge, S.; Werz, O.; Heering, J.; Knapp, S.; Lorkowski, S.; Schubert-Zsilavecz, M.; Merk, D. Endogenous Vitamin E Metabolites Mediate Allosteric PPARγ Activation with Unprecedented Co-Regulatory Interactions. *Cell Chem. Biol.* **2021**, *28* (10), 1489-1500.e8.

(2) Fang, L.; Zhang, M.; Li, Y.; Liu, Y.; Cui, Q.; Wang, N. PPARgene: A Database of Experimentally Verified and Computationally Predicted PPAR Target Genes. *PPAR Res.* **2016**, 6042162.

(3) Santilli, A. A.; Scotese, A. C.; Tomarelli, R. M. A Potent Antihypercholesterolemic Agent: [4-Chloro-6-(2,3-Xylidino)-2-Pyrimidinylthio]Acetic Acid (Wy-14643). *Experientia* **1974**, *30* (10), 1110–1111.

(4) Pollinger, J.; Gellrich, L.; Schierle, S.; Kilu, W.; Schmidt, J.; Kalinowsky, L.; Ohrndorf, J.; Kaiser, A.; Heering, J.; Proschak, E.; Merk, D. Tuning Nuclear Receptor Selectivity of Wy14,643 towards Selective Retinoid X Receptor Modulation. *J. Med. Chem.* **2019**, *62* (4), 2112–2126.

(5) Kabsch, W. Processing of X-Ray Snapshots from Crystals in Random Orientations. *Acta Crystallogr. Sect. D Biol. Crystallogr.* **2014**, *70* (8), 2204–2216.

(6) Evans, P. R.; Murshudov, G. N. How Good Are My Data and What Is the Resolution? *Acta Crystallogr. D. Biol. Crystallogr.* **2013**, *69* (Pt 7), 1204–1214.

(7) Sliwiak, J.; Jaskolski, M.; Dauter, Z.; McCoy, A. J.; Read, R. J. Likelihood-Based Molecular-Replacement Solution for a Highly Pathological Crystal with Tetartohedral Twinning and Sevenfold Translational Noncrystallographic Symmetry. *Acta Crystallogr. Sect. D Biol. Crystallogr.* **2014**, *70* (2), 471–480.

(8) Gellrich, L.; Heitel, P.; Heering, J.; Kilu, W.; Pollinger, J.; Goebel, T.; Kahnt, A.; Arifi, S.; Pogoda, W.; Paulke, A.; Steinhilber, D.; Proschak, E.; Wurglics, M.; Schubert-Zsilavecz, M.; Chaikuad, A.; Knapp, S.; Bischoff, I.; Fürst, R.; Merk, D. L-Thyroxin and the Nonclassical Thyroid Hormone TETRAC Are Potent Activators of PPARγ. *J. Med. Chem.* **2020**, *63* (13), 6727–6740.

(9) Casañal, A.; Lohkamp, B.; Emsley, P. Current Developments in Coot for Macromolecular Model Building of Electron Cryo-Microscopy and Crystallographic Data. *Protein Sci.* **2020**, *29* (4), 1069–1078.

(10) Kovalevskiy, O.; Nicholls, R. A.; Long, F.; Carlon, A.; Murshudov, G. N. Overview of Refinement Procedures within REFMAC 5: Utilizing Data from Different Sources. *Acta Crystallogr. Sect. D Struct. Biol.* **2018**, *74* (Pt 3), 215–227.

(11) Kilu, W.; Merk, D.; Steinhilber, D.; Proschak, E.; Heering, J. Heterodimer Formation with Retinoic Acid Receptor RXRα Modulates Coactivator Recruitment by Peroxisome Proliferator-Activated Receptor PPARγ. *J. Biol. Chem.* **2021**, *297* (1), 100814.

(12) Gellrich, L.; Heitel, P.; Heering, J.; Kilu, W.; Pollinger, J.; Goebel, T.; Kahnt, A.; Arifi, S.; Pogoda, W.; Paulke, A.; Steinhilber, D.; Proschak, E.; Wurglics, M.; Schubert-Zsilavecz, M.; Chaikuad, A.; Knapp, S.; Bischoff, I.; Fürst, R.; Merk, D. L-Thyroxin and the Nonclassical Thyroid Hormone TETRAC Are Potent Activators of PPARγ. *J. Med. Chem.* **2020**, *63* (13), 6727–6740.

(13) Niesen, F. H.; Berglund, H.; Vedadi, M. The Use of Differential Scanning Fluorimetry to Detect Ligand Interactions That Promote Protein Stability. *Nat. Protoc.* **2007**, *2* (9), 2212–2221.

(14) Flesch, D.; Cheung, S.-Y.; Schmidt, J.; Gabler, M.; Heitel, P.; Kramer, J. S.; Kaiser, A.; Hartmann, M.; Lindner, M.; Lüddens-Dämgen, K.; Heering, J.;

Lamers, C.; Lüddens, H.; Wurglics, M.; Proschak, E.; Schubert-Zsilavecz, M.; Merk, D. Non-Acidic Farnesoid X Receptor Modulators. *J. Med. Chem.* **2017**, *60* (16), 7199–7205.
(15) Rau, O.; Wurglics, M.; Paulke, A.; Zitzkowski, J.; Meindl, N.; Bock, A.; Dingermann, T.; Abdel-Tawab, M.; Schubert-Zsilavecz, M. Carnosic Acid and Carnosol, Phenolic Diterpene Compounds of the Labiate Herbs Rosemary and Sage, Are Activators of the Human Peroxisome Proliferator-Activated Receptor Gamma. *Planta Med.* **2006**, *72* (10), 881–887.
(16) Moret, M.; Helmstädter, M.; Grisoni, F.; Schneider, G.; Merk, D. Beam Search for Automated Design and Scoring of Novel ROR Ligands with Machine Intelligence**. *Angew. Chemie - Int. Ed.* **2021**, *60* (35), 19477–19482.
(17) Heitel, P.; Achenbach, J.; Moser, D.; Proschak, E.; Merk, D. DrugBank Screening Revealed Alitretinoin and Bexarotene as Liver X Receptor Modulators. *Bioorg. Med. Chem. Lett.* **2017**, *27* (5), 1193–1198.
(18) Schmidt, J.; Klingler, F.-M.; Proschak, E.; Steinhilber, D.; Schubert-Zsilavecz, M.; Merk, D. NSAIDs Ibuprofen, Indometacin, and Diclofenac Do Not Interact with Farnesoid X Receptor. *Sci. Rep.* **2015**, *5*, 14782.
(19) Meijer, I.; Willems, S.; Ni, X.; Heering, J.; Chaikuad, A.; Merk, D. Chemical Starting Matter for HNF4α Ligand Discovery and Chemogenomics. *Int. J. Mol. Sci.* **2020**, *21*, 7895.
(20) Heitel, P.; Gellrich, L.; Kalinowsky, L.; Heering, J.; Kaiser, A.; Ohrndorf, J.; Proschak, E.; Merk, D. Computer-Assisted Discovery and Structural Optimization of a Novel Retinoid X Receptor Agonist Chemotype. *ACS Med. Chem. Lett.* **2019**, *10* (2), 203–208.
(21) Faudone, G.; Zhubi, R.; Celik, F.; Knapp, S.; Chaikuad, A.; Heering, J.; Merk, D. Design of a Potent TLX Agonist by Rational Fragment Fusion. *J. Med. Chem.* **2022**, *65* (3), 2288–2296.
(22) Willems, S.; Kilu, W.; Ni, X.; Chaikuad, A.; Knapp, S.; Heering, J.; Merk, D. The Orphan Nuclear Receptor Nurr1 Is Responsive to Non-Steroidal Anti-Inflammatory Drugs. *Commun. Chem.* **2020**, *3*, 85.
(23) Wolbank, S.; Stadler, G.; Peterbauer, A.; Gillich, A.; Karbiener, M.; Streubel, B.; Wieser, M.; Katinger, H.; Van Griensven, M.; Redl, H.; Gabriel, C.; Grillari, J.; Grillari-Voglauer, R. Telomerase Immortalized Human Amnion- and Adipose-Derived Mesenchymal Stem Cells: Maintenance of Differentiation and Immunomodulatory Characteristics. *Tissue Eng. Part A* **2009**, *15* (7), 1843–1854.
(24) Mortazavi, A.; Williams, B. A.; McCue, K.; Schaeffer, L.; Wold, B. Mapping and Quantifying Mammalian Transcriptomes by RNA-Seq. *Nat. Methods* **2008**, *5* (7), 621–628.